# Search for supersymmetry in proton-proton collisions at 13 TeV using identified top quarks

A. M. Sirunyan *et al.*[*]

(CMS Collaboration)

A search for supersymmetry is presented based on proton-proton collision events containing identified hadronically decaying top quarks, no leptons, and an imbalance $p_T^{\text{miss}}$ in transverse momentum. The data were collected with the CMS detector at the CERN LHC at a center-of-mass energy of 13 TeV, and correspond to an integrated luminosity of 35.9 fb$^{-1}$. Search regions are defined in terms of the multiplicity of bottom quark jet and top quark candidates, the $p_T^{\text{miss}}$, the scalar sum of jet transverse momenta, and the $m_{T2}$ mass variable. No statistically significant excess of events is observed relative to the expectation from the standard model. Lower limits on the masses of supersymmetric particles are determined at 95% confidence level in the context of simplified models with top quark production. For a model with direct top squark pair production followed by the decay of each top squark to a top quark and a neutralino, top squark masses up to 1020 GeV and neutralino masses up to 430 GeV are excluded. For a model with pair production of gluinos followed by the decay of each gluino to a top quark-antiquark pair and a neutralino, gluino masses up to 2040 GeV and neutralino masses up to 1150 GeV are excluded. These limits extend previous results.

## I. INTRODUCTION

The observation [1–3] of a Higgs boson ($H$) has been the most significant discovery to date at the CERN LHC. However, its relatively small mass of about 125 GeV [4] can be understood in the context of the standard model (SM) only through fine tuning of the associated quantum loop corrections [5]. A compelling model that can account for the observed Higgs boson mass without this fine tuning is the extension to the SM called supersymmetry (SUSY) [6–14]. The main assertion of SUSY is the existence of one or more particles, called superpartners, for every SM particle, where the spin of a superpartner differs from that of its SM counterpart by a half integer. The superpartners of quarks, gluons, and Higgs bosons are squarks $\tilde{q}$, gluinos $\tilde{g}$, and Higgsinos, respectively, while neutralinos $\tilde{\chi}^0$ and charginos $\tilde{\chi}^{\pm}$ are mixtures of the superpartners of electroweak and Higgs bosons. In so-called natural models of SUSY [15], the top squark, bottom squark, gluino, and Higgsinos are required to have masses no larger, and often much smaller, than a few TeV, motivating searches for these particles at the LHC.

In this paper we present a search for top squarks and gluinos. The data were collected in 2016 by the CMS experiment at the LHC and correspond to an integrated luminosity of 35.9 fb$^{-1}$ of proton-proton ($pp$) collisions at a center-of-mass energy of 13 TeV. The search is performed in all-hadronic events with a large imbalance $p_T^{\text{miss}}$ in transverse momentum, where by "all-hadronic" we mean that the final states are composed solely of hadronic jets. Recent searches for SUSY in a similar final state are presented in Refs. [16–20]. The current analysis is distinguished by the requirement that identified ("tagged") hadronically decaying top quarks be present. It represents an extension, using improved analysis techniques and a data sample 16 times larger, of the study in Ref. [20].

In the search, top squarks are assumed to be produced either through the direct production of a top squark-antisquark pair or in the decay of pair-produced gluinos. They are assumed to decay to the lightest neutralino $\tilde{\chi}_1^0$—taken to be a stable, weakly interacting, lightest SUSY particle (LSP)—and a quark. Since the LSP interacts only weakly, it does not produce a signal in the detector, thus generating $p_T^{\text{miss}}$. A novel top quark tagging algorithm is employed to identify hadronically decaying top quarks produced in the decay chains. The algorithm makes use of the facts that a top quark essentially always decays to a bottom quark and a $W$ boson, and that—in hadronic decays—the $W$ boson decays to a quark-antiquark ($q\bar{q}'$) pair. The algorithm recognizes three different types of decay topology for the top quark. In order of increasing Lorentz boost for the top quark, these are: (i) three distinct jets with no more than one of them identified as a bottom quark jet ("$b$ jet"), where two non-$b$ jets arise from the $q$

and $\bar{q}'$ produced in the $W$ boson decay; (ii) two distinct jets, one of which corresponds to the $b$ quark and the other to the merged $q\bar{q}'$ decay products from the $W$ boson; and (iii) a single jet representing the merged decay products of the $b$ quark and $W$ boson. By accounting for these three different topologies, the algorithm achieves high detection efficiency over a wide range of top quark transverse momentum $p_T$.

Events are selected that contain large $p_T^{miss}$, at least four jets, at least one identified $b$ jet, at least one identified top quark, and no identified leptons. Search regions are defined based on the number $N_b$ of identified $b$ jets, the number $N_t$ of top quark candidates, the $p_T^{miss}$, the scalar sum $H_T$ of the $p_T$ of jets, and the $m_{T2}$ [21,22] mass variable, where $m_{T2}$ is calculated using the reconstructed top quarks.

The largest source of SM background arises from top quark-antiquark pair ($t\bar{t}$), single top quark, and $W$ + jets production, namely from events in which a leptonically decaying $W$ boson yields both a high-momentum neutrino, generating $p_T^{miss}$, and a charged lepton that is either not identified, not reconstructed, or outside the analysis acceptance. Another important source of background is $Z$ + jets production followed by $Z \rightarrow \nu\bar{\nu}$ decay. Quantum chromodynamics (QCD) multijet events, namely events with multijet final states produced exclusively through the strong interaction, can contribute to the background if mismeasurement of jet $p_T$ yields large reconstructed $p_T^{miss}$ or if a semileptonically decaying charm or bottom hadron is produced. Events with $t\bar{t}$ production in which both top quarks decay hadronically are indistinguishable from QCD multijet events and are included in the QCD multijet background. Because of the relatively small $t\bar{t}$ cross section, these $t\bar{t}$ events constitute only a few percent of the evaluated QCD multijet background. Small sources of background include multiple vector boson production and events with a $t\bar{t}$ pair produced in association with a $Z$ boson.

## II. SIGNAL MODELS

Signal scenarios for SUSY are considered in the context of simplified models [23–27]. For direct top squark pair production, the simplified model denoted "T2tt" is examined. In this model, each top squark $\tilde{t}$ decays to a top quark and the LSP: $\tilde{t} \rightarrow t\tilde{\chi}_1^0$. For top squark production through gluino decay, the models described in the following two paragraphs are considered.

In the model denoted "T1tttt," pair-produced gluinos each decay to an off-shell top squark and an on-shell top quark. The off-shell top squark decays to a top quark and the LSP. The gluino decay is thus $\tilde{g} \rightarrow t\bar{t}\tilde{\chi}_1^0$. The T1tttt model provides sensitivity to situations in which the top squark is too heavy to be produced directly while the gluino is not. In the "T1ttbb" model, pair-produced gluinos each decay via an off-shell top or bottom squark as $\tilde{g} \rightarrow t\bar{t}\tilde{\chi}_1^0$ (25%), $\tilde{g} \rightarrow \bar{t}b\tilde{\chi}_1^+$ or its charge conjugate (50%), or $\tilde{g} \rightarrow b\bar{b}\tilde{\chi}_1^0$ (25%),

where $\tilde{\chi}_1^+$ is the lightest chargino. The mass difference between the $\tilde{\chi}_1^+$ and the LSP is taken to be $\Delta m(\tilde{\chi}_1^+, \tilde{\chi}_1^0) = 5$ GeV. Thus the $\tilde{\chi}_1^+$ is taken to be nearly mass degenerate with the $\tilde{\chi}_1^0$, representing the expected situation should the two particles appear within the same SU(2) multiplet [25]. The $\tilde{\chi}_1^+$ subsequently decays to the LSP and an off-shell $W$ boson. The T1ttbb model provides sensitivity to mixed states of top and bottom squarks.

In the model denoted "T5tttt," the mass difference between the top squark and the LSP is $\Delta m(\tilde{t}, \tilde{\chi}_1^0) = 175$ GeV. Pair-produced gluinos each decay to a top quark and an on-shell top squark. The top squark decays to a top quark and the LSP. This model provides sensitivity to a region that is difficult to probe with the T2tt model because of the similarity between the properties of T2tt signal and $t\bar{t}$ background events when $\Delta m(\tilde{t}, \tilde{\chi}_1^0)$ approximately equals the top quark mass ($m_t$). The "T5ttcc" model is similar to the T5tttt model except it assumes $\Delta m(\tilde{t}, \tilde{\chi}_1^0) = 20$ GeV and the top squark decays to a charm quark and the LSP. Note that decay to a charm quark and an LSP represents the dominant decay mode of a top squark when its decay to a top quark and an LSP is kinematically disallowed. The choice of $\Delta m(\tilde{t}, \tilde{\chi}_1^0)$ has little effect on the final results for the T5ttcc model (Sec. X) so long as $\Delta m(\tilde{t}, \tilde{\chi}_1^0)$ remains below $m_t$. The T5ttcc model provides sensitivity to scenarios in which the top squark is kinematically unable to decay to an on-shell top quark.

The signal scenarios are illustrated in Fig. 1. They exhibit common features, such as the presence of multiple top quarks and two LSPs.
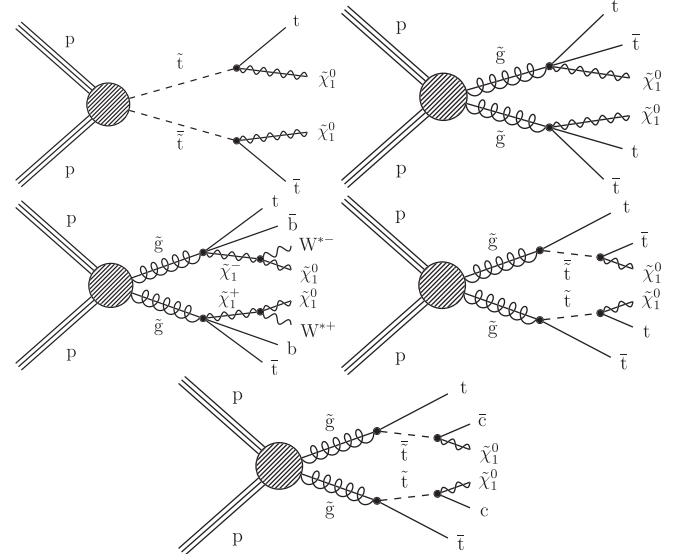


FIG. 1.   Diagrams representing the simplified models of direct and gluino-mediated top squark production considered in this study: the T2tt model (top left), the T1tttt model (top right), the T1ttbb model (middle left), the T5tttt (middle right), and the T5ttcc model (bottom).

## III. THE CMS DETECTOR

The CMS detector is built around a superconducting solenoid of $6m$ internal diameter, which provides a magnetic field of 3.8 T. Within the solenoid volume are a silicon pixel and strip tracker, a lead tungstate crystal electromagnetic calorimeter (ECAL), and a brass and scintillator hadron calorimeter (HCAL). The tracking detectors extend over the pseudorapidity range $|\eta| < 2.5$. The ECAL and HCAL, each composed of a barrel and two endcap sections, cover $|\eta| < 3.0$. Forward calorimeters on each side of the interaction point encompass $3.0 < |\eta| < 5.2$. Muons are detected within $|\eta| < 2.4$ by gas-ionization chambers embedded in a steel magnetic flux-return yoke outside the solenoid. A more detailed description of the CMS detector, together with a definition of the coordinate system used and the relevant kinematic variables, can be found in Ref. [28].

Events are selected using a two-level trigger system [29]. The first level, composed of custom hardware processors, uses information from the calorimeters and muon detectors to select events of interest at a rate of around 100 kHz. The second level, composed of a high-level processor farm, decreases the event rate to around 1 kHz before data storage.

For the present analysis, events in the search regions are collected with a trigger that requires $p_T^{miss} > 100$ GeV and $H_T^{miss} > 100$ GeV, where $H_T^{miss}$ is the magnitude of the vector $p_T$ sum of jets reconstructed at the trigger level. This trigger is fully efficient after application of the event selection criteria described below.

## IV. EVENT RECONSTRUCTION

Events are reconstructed using the particle-flow (PF) algorithm [30], which reconstructs charged hadrons, neutral hadrons, photons, electrons, and muons using information from all subdetectors. Electron and muon candidates are subjected to additional requirements [31,32] to improve their purity, and are further required to have $p_T > 10$ GeV and to originate from within 2 mm of the beam axis in the transverse plane. Electron (muon) candidates must appear within $|\eta| < 2.5$ (2.4). The missing transverse momentum $\vec{p}_T^{miss}$ in an event is given by the negative of the vector $p_T$ sum of all reconstructed objects. Its magnitude is denoted $p_T^{miss}$.

All photons and neutral hadrons in an event, together with charged particles that originate from the primary interaction vertex, are clustered into jets using the anti-$k_T$ algorithm with a distance parameter of 0.4 (AK4) [33]. The jets must satisfy a set of jet identification criteria as specified in Ref. [34]. Neutral particles from overlapping $pp$ interactions ("pileup") are subtracted on an event-by-event basis using the FASTJET technique [35,36]. Jets are corrected using factors from simulation to account for detector response as a function of jet $p_T$ and $\eta$. Additional

corrections account for residual differences between simulation and data for the jet energy and momentum scales [37]. Only jets with $p_T > 30$ GeV and either $|\eta| < 2.4$ (tight) or $|\eta| < 5.0$ (loose) are retained. The number of jets $N_j$ in an event is defined to be the number of tight AK4 jets. The $H_T$ variable is given by the scalar sum of jet $p_T$ over this same jet sample.

Bottom quark jets are identified ($b$ tagged) by applying the combined secondary vertex algorithm (CSVv2) [38,39] at the medium working point to tight AK4 jets. The $b$ quark identification efficiency ranges from 60 to 70% for jet $p_T$ between 20 and 400 GeV. The probability for a jet originating from a gluon or light-flavored quark to be $b$ tagged, averaged over the jets in a sample of $t\bar{t}$ events, is 1.4% [38].

In addition to AK4 jets, we define AK8 jets, constructed by clustering PF objects using the anti-$k_T$ algorithm with a distance parameter of 0.8. The AK8 jets are used in the top quark reconstruction procedure, described in Sec. VII. Pileup contributions to AK8 jets are accounted for using the "pileup per particle identification" [40,41] method, by which each charged and neutral particle is weighted by a factor representing its probability to originate from the primary interaction vertex before the clustering is performed. The AK8 jets are required to satisfy $p_T > 200$ GeV.

## V. LEPTON AND TRACK VETOES

To obtain an all-hadronic event sample, events with isolated electrons or muons are vetoed. The isolation of electron and muon candidates is defined as the scalar $p_T$ sum of PF candidates in a cone of radius $\Delta R = \sqrt{(\Delta\eta)^2 + (\Delta\phi)^2}$ around the candidate's trajectory, where $\phi$ is the azimuthal angle and the sum excludes the electron or muon candidate. The cone size is 0.2 for $p_T \leq 50$ GeV, 0.05 for $p_T \geq 200$ GeV, and decreases in inverse proportion to the lepton $p_T$ for $50 < p_T < 200$ GeV. This decrease in cone size with increasing lepton $p_T$ accounts for the greater collimation of a heavy object's decay products as its Lorentz boost increases. The isolation sum is corrected for contributions from pileup using an estimate of the pileup energy in the cone [35]. Electron and muon candidates are considered to be isolated if their relative isolation, i.e., the ratio of the isolation sum to the candidate $p_T$, is less than 0.1 and 0.2, respectively.

Events that survive the lepton veto are subjected to an isolated charged-particle track veto. This veto suppresses events with a hadronically decaying $\tau$ lepton or with an isolated electron or muon not identified as such. Tracks considered for this veto must have $p_T > 5$ GeV, $|\eta| < 2.5$, and relative track isolation less than 0.2. The relative track isolation is defined analogously to the relative isolation of electrons and muons but is computed using charged PF candidates only, that appear within a fixed cone of

$\Delta R = 0.3$ around the track. To preserve signal efficiency, the isolated-track veto is applied only if the transverse mass $m_T$ [42] of the isolated track-$\vec{p}_T^{miss}$ system is consistent with $W$ boson decay, namely $m_T < 100$ GeV. The isolated-track veto reduces background from events with a leptonically decaying $W$ boson by about 40%.

Following application of the above two vetoes, a significant fraction of the remaining SM background arises from events with a hadronically decaying $\tau$ lepton ($\tau_h$). A charged-hadron veto is applied to reduce this background. The charged-hadron veto eliminates events that contain an isolated PF charged hadron with $p_T > 10$ GeV, $|\eta| < 2.5$, and $m_T < 100$ GeV. To be considered isolated, the relative isolation of the charged hadron, defined as in the previous paragraph, must be less than 0.1.

## VI. EVENT SIMULATION

Samples of Monte Carlo (MC) simulated events are used to study the properties of signal and background processes. The MADGRAPH5_aMC@NLO 2.2.2 [43,44] event generator at leading-order (LO) is used to describe signal events and the SM production of $t\bar{t}$, $W$ + jets (with $W \to \ell\nu$), $Z$ + jets (with $Z \to \nu\bar{\nu}$), Drell–Yan (DY) + jets, and QCD multijet events. The $t\bar{t}$ events are generated with up to three additional partons present beyond those that participate in the hard scattering, the signal events with up to two, and the other processes with up to four. The DY + jets events, specifically events with the decay of a real or virtual $Z$ boson to a $\mu^+\mu^-$ pair, are used as part of the procedure to evaluate background (Sec. IX B). The generation of these processes is based on LO parton distribution functions (PDFs) from NNPDF3.0 [45]. Single top quark events in the $tW$ channel are generated with the next-to-leading order (NLO) POWHEG v2.0 [46–49] program. The following rare SM processes are considered: $t\bar{t}Z$, $t\bar{t}W$, triboson, and $t\bar{t}H$ production, generated at NLO with the MADGRAPH5_aMC@NLO 2.2.2 [43,50] program using NLO NNPDF3.0 PDFs; $WZ$ and $ZZ$ production, generated either with this same program or with the POWHEG program mentioned in the previous sentence depending on the decay mode; and $WW$ production, generated with the POWHEG program mentioned in the previous sentence. Parton showering and hadronization are simulated for all MC samples with the PYTHIA v8.205 [51] program, which uses the underlying event tune CUETP8M1 [52].

For simulated background processes, the CMS detector response is based on the GEANT4 package [53]. Because of the intense computational requirements, the detector response for simulated signal events is performed with a fast simulation [54], which is tuned to provide results that are consistent with those from the GEANT4-based simulation. For all MC samples, event reconstruction is performed in the same manner as for the data.

The signal production cross sections are calculated using NLO plus next-to-leading logarithm (NLL) calculations [55]. The most precise cross section calculations currently available are used to normalize the SM simulated samples, corresponding to NLO or next-to-NLO accuracy in most cases [43,56–62].

The simulated events are corrected for differences between simulation and data in the $b$ tagging efficiency, the top quark tagging (Section VII) efficiency, and the electron and muon identification and isolation selection efficiencies. The corrections for the $b$ tagging efficiency are derived from multijet- and $t\bar{t}$-enriched event samples and are parameterized in terms of the jet kinematics [38]. The corrections for the top quark tagging efficiency are derived from a single-muon $t\bar{t}$-enriched control sample and are applied as a function of top quark $p_T$. The corrections for the electron and muon identification and isolation efficiencies are determined from $Z \to \ell\ell$ events.

Simulated $t\bar{t}$ and signal events are corrected with scale factors to account for imperfect modeling of initial-state radiation (ISR). The ISR corrections are derived from a $t\bar{t}$-enriched control sample containing two leptons ($ee$, $\mu\mu$, or $e\mu$) and two tagged $b$ jets, and are applied as a function of $N_{jet}^{ISR}$ up to $N_{jet}^{ISR} = 6$, where $N_{jet}^{ISR}$ is the number of jets in the event other than the two that are $b$ tagged. The correction is validated by applying it to simulation in a $t\bar{t}$-dominated single-lepton control sample covering various regions of phase space, including regions with a large number of jets. Agreement with data on the level of 20% of the correction is found in this control sample for key observables such as the distribution in the number of jets. To account for possible differences between $t\bar{t}$ and signal events, a conservative uncertainty of 50% of the correction is assigned to the scale factors, both as applied to $t\bar{t}$ and signal processes.

## VII. TOP QUARK RECONSTRUCTION

The top quark tagging algorithm is the central feature of our analysis. It is designed to provide high reconstruction efficiency over the full range of top quark $p_T$ in the considered signal models. A common strategy [63,64] for tagging hadronically decaying top quarks is to cluster jets with the AK8 algorithm and then to test whether the jet is consistent with having three subjets, as expected for the $t \to bq\bar{q}'$ decay of a highly Lorentz-boosted top quark. Although these algorithms are efficient at large top quark $p_T$, for $p_T < 400$ GeV top quarks are more efficiently reconstructed by combining three individual AK4 jets, an approach known as "resolved" top quark tagging. To obtain high reconstruction efficiency over a wide range of top quark $p_T$, we employ both types of algorithms and, in addition, consider top quark decays in which the decay products of the $W$ boson are contained within an AK8 jet. To fully reconstruct the top quark in the latter case, an AK8 jet corresponding to the $W$ boson decay is combined with an AK4 jet.

To identify high-$p_T$ top quarks, AK8 jets with $p_T >$ 400 GeV are selected. The mass of the jet is corrected with the soft-drop method [65,66] using angular exponent $\beta = 0$, soft cutoff threshold $z_{cut} < 0.1$, and characteristic radius $R_0 = 0.8$, where the values of $\beta$, $z_{cut}$, and $R_0$ are those recommended in Ref. [67] for AK8 jets. The soft-drop algorithm reclusters the AK8 jet into subjets using the Cambridge–Aachen algorithm [68,69]. This reclustering removes soft radiation, which can bias the jet mass determination. To be considered as a top quark candidate, the soft-drop mass must lie between 105 and 210 GeV. The $N$-subjettiness variables $\tau_N$ [70] are used to determine the consistency of the jet with having three subjets. More details on this algorithm can be found in Ref. [63]. To be consistent with having three subjets, the requirement $\tau_3/\tau_2 < 0.65$ is imposed. This requirement is made on the basis of optimization studies [67].

To avoid overlap between the top-tagged AK8 jets (denoted "monojets") and the AK4 jets that are used to reconstruct resolved ("trijets") or partially merged ("dijets") top quarks, AK4 jets matched to the top-tagged AK8 jet are removed from the list of AK4 jets used in the reconstruction of the dijet and trijet categories. An AK4 jet is considered matched if it lies within $\Delta R < 0.4$ of one of the soft-drop subjets of the tagged AK8 jet.

For the dijet category of top quark decays, we employ a similar technique to identify the jet from the hadronic $W$ boson decay. An AK8 jet with $p_T > 200$ GeV must have a soft-drop corrected mass between 65 and 100 GeV. To be consistent with having two subjets, the requirement $\tau_2/\tau_1 < 0.6$ is imposed. This requirement corresponds to the "high-purity pruning" criterion of Ref. [67]. The AK8 jet is combined with a loose AK4 jet to form a top quark candidate. The candidate must have a mass between 100 and 250 GeV, both jets must appear within a cone of radius $\Delta R = 1$ around the direction of their summed $p_T$ vector, and the ratio of the soft-drop corrected AK8 jet mass to the top quark candidate mass must lie between $0.85(m_W/m_t)$ and $1.25(m_W/m_t)$, with $m_W$ the $W$ boson mass. If more than one top quark candidate is found using the same AK8 jet, the combination with mass closest to $m_t$ is chosen. The AK4 jet used to form the top quark candidate, and all AK4 jets matched to within $\Delta R < 0.4$ of the soft-drop subjets from the AK8 jet, are removed from the list used to reconstruct the trijet category.

The trijet sample of top quark candidates is formed by combining three loose AK4 jets. The three jets must appear within a cone of radius $\Delta R = 1.5$ around the direction of their summed $p_T$ vector, no more than one of the three jets can be $b$ tagged, and the trijet mass must lie between 100 and 250 GeV. The cone size is chosen to be $\Delta R = 1.5$ because the background becomes very large for larger $\Delta R$ values. The final trijet top quark sample is defined by applying the results of a random forest boosted decision tree [71] to the selected combinations. The random forest is trained with simulation using trijet combinations that satisfy the above criteria. Simulated samples of $t\bar{t}$ and $Z(\nu\bar{\nu}) +$ jets events are used for this purpose. In the $t\bar{t}$ simulation, one top quark decays hadronically and the other semileptonically. Signal top quarks are defined as trijet combinations in the $t\bar{t}$ simulation for which each of the three jets is matched to a distinct generator-level hadronically decaying top quark decay product within $\Delta R < 0.4$, and whose overall momentum is matched to the generator-level top quark momentum within $\Delta R < 0.6$. Background combinations are defined as trijet combinations in the $t\bar{t}$ sample with no jet matched to a generator-level hadronically decaying top quark decay product, and as trijet combinations in the $Z(\nu\bar{\nu}) +$ jets sample. If more than one background combination is found in an event, all combinations are used.

The variables considered in the random forest algorithm are the mass of the trijet system, the mass of each dijet combination, the angular separation and momenta of the jets in the trijet rest frame, the $b$ tagging discriminator value of each jet, and the quark-versus-gluon-jet discriminator [72] value of each jet. To reduce correlations with the top quark $p_T$ and thus to prevent overtraining in this variable, the $p_T$ spectra of signal and background triplet combinations are flattened through reweighting. The random forest performance is improved by replacing the kinematic variables in the laboratory frame with their equivalents in the trijet rest frame, and by sorting jets according to their momenta in the trijet rest frame so that the highest (lowest) momentum jet is most (least) likely to originate from a $b$ quark.

Trijet top quark candidates are selected by requiring the random forest discriminator value to exceed 0.85. This value is chosen based on optimization studies involving the full limit-setting procedure described in Sec. X. If two or more selected trijets share one or more AK4 jets, only the combination with the largest discriminator value is retained.

All top quark candidates must have $|\eta| < 2.0$. The final set consists of the nonoverlapping candidates from the three reconstruction categories. The total efficiency of the algorithm, including a breakdown into the three categories, is shown in Fig. 2. The efficiency is determined using T2tt signal events with a top squark mass of 850 GeV and an LSP mass of 100 GeV, based on the number of generator-level hadronically decaying top quarks that are matched to a reconstructed top quark candidate divided by the total number of generator-level top quarks that decay hadronically. Similar results are found using SM $t\bar{t}$ events. The matching between the generator-level and reconstructed top quarks requires the overall reconstructed top quark to be matched to the generator-level top quark within $\Delta R < 0.4$. The misidentification rate varies between 15 and 22% as a function of $p_T^{miss}$, with an average of about 20%, as determined using simulated $Z(\nu\bar{\nu}) +$ jets events after
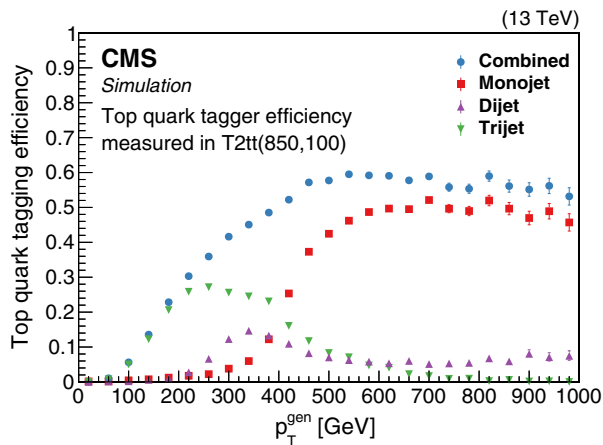
FIG. 2. Efficiency of the top quark tagger as a function of generator-level top quark $p_T$ for the monojet (red boxes), dijet (magenta triangles), and trijet (green upside-down triangles) categories and for their combination (blue circles), as determined using T2tt signal events with a top squark mass of 850 GeV and an LSP mass of 100 GeV. The vertical bars indicate the statistical uncertainties.

applying selection criteria similar to those used for the data (Sec. VIII): $N_j \geq 4$, $N_b \geq 1$, $p_T^{\mathrm{miss}} > 250$ GeV, and no isolated electron or muon with $p_T > 10$ GeV.

Relative to Ref. [20], the top quark tagging algorithm has been improved by using AK8 jets for the monojet and dijet categories, rather than strictly AK4 jets, and through implementation of the random forest tree for the trijet category. These improvements provide a factor of two reduction in the top quark misidentification rate while maintaining a similar efficiency.

## VIII. EVENT SELECTION AND SEARCH REGIONS

Our study is an inclusive search for events containing $p_T^{\mathrm{miss}}$ and reconstructed top quarks. The selection criteria are intended, in general, to be nonrestrictive, while still providing high trigger efficiency and sensitivity to a wide variety of new-physics scenarios. All events must satisfy filters designed to remove detector- and beam-related noise. The events are subjected to the lepton, isolated-track, and charged-hadron vetoes of Sec. V. To improve the rejection of background, the two tight AK4 jets with highest $p_T$ must have $p_T > 50$ GeV. Events are required to have $N_j \geq 4$, $N_b \geq 1$, $N_t \geq 1$, $p_T^{\mathrm{miss}} > 250$ GeV, and $H_T > 300$ GeV.

The QCD multijet background mostly arises when the $p_T$ of one of the highest $p_T$ jets is undermeasured, causing $\vec{p}_T^{\mathrm{miss}}$ to be aligned with that jet. This undermeasurement can occur because of jet misreconstruction or, in the case of semileptonic $b$ or $c$ quark decays, an undetected neutrino. To reduce this background, requirements are placed on the azimuthal angle between $\vec{p}_T^{\mathrm{miss}}$ and the three loose AK4 jets with highest $p_T$, denoted $j_1$, $j_2$, and $j_3$ in order of decreasing $p_T$. Specifically, we require $\Delta\phi(\vec{p}_T^{\mathrm{miss}}, j_1) > 0.5$, $\Delta\phi(\vec{p}_T^{\mathrm{miss}}, j_2) > 0.5$, and $\Delta\phi(\vec{p}_T^{\mathrm{miss}}, j_3) > 0.3$.

The $m_{\mathrm{T2}}$ variable [20–22] is used to reduce background from $t\bar{t}$ events. This variable is designed to provide an estimate of the transverse mass of pair-produced heavy objects that decay to both visible and undetected particles. It has a kinematic upper limit at the mass of the heavy object undergoing decay. Thus the upper limit for SM $t\bar{t}$ events is $m_t$, while the upper limit for TeV-scale squarks and gluinos is much larger. If there are two tagged top quarks in an event, $m_{\mathrm{T2}}$ is calculated using the pair of tagged top quarks and $\vec{p}_T^{\mathrm{miss}}$. If there are more than two tagged top quarks, we compute $m_{\mathrm{T2}}$ for all combinations and choose the combination with the smallest $m_{\mathrm{T2}}$. If there is only one tagged top quark, we construct a proxy for the other top quark using the highest $p_T$ $b$ tagged jet as a seed. If a $b$ tagged jet is not available, because there is only one $b$ tagged jet in the event and it is part of the reconstructed top quark, the highest $p_T$ jet is used as the seed. The seed jet is combined with a loose AK4 jet to define the top quark proxy if the resulting pair of jets has a mass between 50 and 220 GeV and if the two jets appear within $\Delta R = 1.5$ of each other; otherwise the seed jet by itself is used as the top quark proxy. The proxy is combined with the tagged top quark and $\vec{p}_T^{\mathrm{miss}}$ to determine $m_{\mathrm{T2}}$. Irrespective of the number of tagged top quarks, we require $m_{\mathrm{T2}} > 200$ GeV.

The search is performed in 84 nonoverlapping search regions. Regions with $N_b \leq 2$ and $N_t \leq 2$ use $N_b$, $N_t$, $p_T^{\mathrm{miss}}$, and $m_{\mathrm{T2}}$ as the binned search variables. Regions with $N_b \geq 3$ or $N_t \geq 3$ use $N_b$, $N_t$, $p_T^{\mathrm{miss}}$, and $H_T$. The reason $H_T$ is used for these latter regions, and not $m_{\mathrm{T2}}$, is that in events with many jets, the jets from the decay of a particular heavy object may not always be correctly associated with that object, causing the distribution of $m_{\mathrm{T2}}$ to be broad and relatively flat. We find that $H_T$ provides better discrimination between signal and background for $N_b \geq 3$ or $N_t \geq 3$. The 84 regions in $m_{\mathrm{T2}}$ versus $p_T^{\mathrm{miss}}$ or in $H_T$ versus $p_T^{\mathrm{miss}}$ are illustrated in Fig. 3. The boundaries between the regions were determined through sensitivity studies.

To simplify use of our data by others, we also define 10 aggregate search regions, specified in Table I. The aggregate regions are nonexclusive and are intended to be considered independently. The first four aggregate regions represent topologies of general interest. The fifth and sixth are sensitive to direct top squark pair production. The seventh region targets the large $\Delta m(\tilde{g}, \tilde{\chi}_1^0)$ region of T5ttcc-like models, while the final three target events with a large number of top quarks such as are produced in the T1tttt and T5tttt models.

## IX. BACKGROUND ESTIMATION

We next discuss the evaluation of the SM background. A change relative to Ref. [20] is that we now use a translation
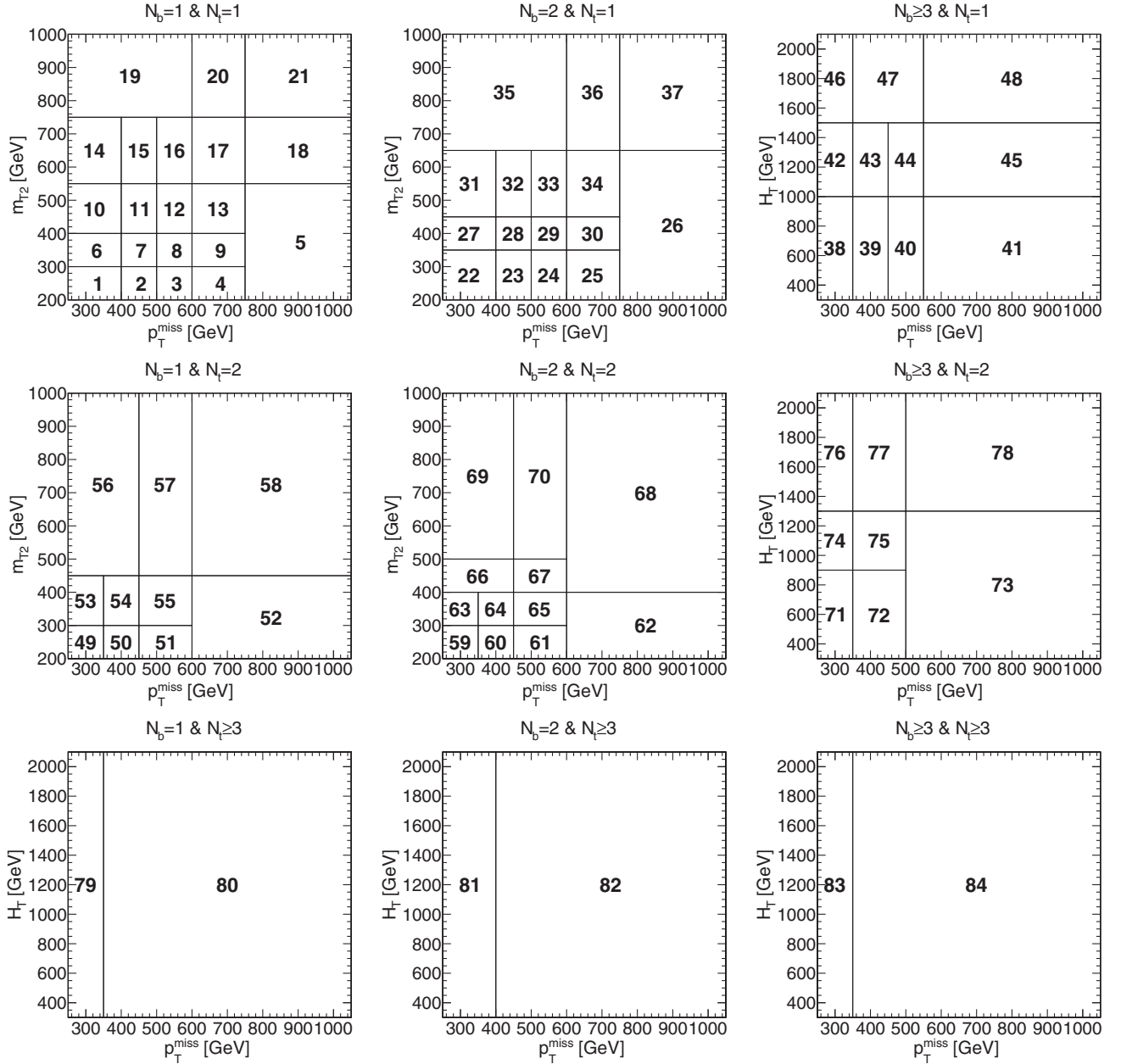
FIG. 3.    Search region definitions in the kinematic variables. The highest $p_T^{miss}$, $m_{T2}$, and $H_T$ regions are open-ended, e.g., $p_T^{miss} >$ 750 GeV and $m_{T2} > 750$ GeV for search region 21.

factor method, as described in Sec. IX A, to evaluate the background from $t\bar{t}$, single top quark, and $W +$ jets events. In Ref. [20] we rather used $\tau_h$ response templates and separately evaluated terms constructed from the electron and muon acceptance, isolation efficiency, and reconstruction-and-identification efficiency to evaluate this background. The reason for the change is to simplify the modeling of variables for the AK8 jets and for the random forest decision tree now used in the top quark tagging algorithm. Another change is that the "loose" dimuon control sample described in Sec. IX B is selected using more restrictive requirements, as is allowed by the larger

data sample now available, leading to reduced systematic uncertainties.

## A. Background from $t\bar{t}$, single top quark, and $W +$ jets events

The largest background, accounting for about 70% of the total background integrated over the 84 search regions, is due to $t\bar{t}$, single top quark, and $W +$ jets events with a leptonically decaying $W$ boson. This background arises in one of two distinct ways. First, if the $W$ boson decays to a $\tau$ lepton that decays hadronically, the $\tau$ lepton can be

TABLE I. Definition of the aggregate search regions.

| Region | $N_t$ | $N_b$ | $m_{T2}$ [GeV] | $p_T^{miss}$ [GeV] | Motivation |
|---|---|---|---|---|---|
| 1 | $\geq 1$ | $\geq 1$ | $\geq 200$ | $\geq 250$ | Events satisfying selection criteria |
| 2 | $\geq 2$ | $\geq 2$ | $\geq 200$ | $\geq 250$ | Events with $N_t \geq 2$ and $N_b \geq 2$ |
| 3 | $\geq 3$ | $\geq 1$ | $\geq 200$ | $\geq 250$ | Events with $N_t \geq 3$ and $N_b \geq 1$ |
| 4 | $\geq 3$ | $\geq 3$ | $\geq 200$ | $\geq 250$ | T5tttt; small $\Delta m(\tilde{g}, \tilde{\chi}_1^0)$ and $m_{\tilde{\chi}_1^0} < m_t$ |
| 5 | $\geq 2$ | $\geq 1$ | $\geq 200$ | $\geq 400$ | T2tt; small $\Delta m(\tilde{t}, \tilde{\chi}_1^0)$ |
| 6 | $\geq 1$ | $\geq 2$ | $\geq 600$ | $\geq 400$ | T2tt; large $\Delta m(\tilde{t}, \tilde{\chi}_1^0)$ |

| Region | $N_t$ | $N_b$ | $H_T$ [GeV] | $p_T^{miss}$ [GeV] | Motivation |
|---|---|---|---|---|---|
| 7 | $\geq 1$ | $\geq 2$ | $\geq 1400$ | $\geq 500$ | T1ttbb & T5ttcc; large $\Delta m(\tilde{g}, \tilde{\chi}_1^0)$ |
| 8 | $\geq 2$ | $\geq 3$ | $\geq 600$ | $\geq 350$ | T1tttt; small $\Delta m(\tilde{g}, \tilde{\chi}_1^0)$ |
| 9 | $\geq 2$ | $\geq 3$ | $\geq 300$ | $\geq 500$ | T1/T5tttt & T1ttbb; intermediate $\Delta m(\tilde{g}, \tilde{\chi}_1^0)$ |
| 10 | $\geq 2$ | $\geq 3$ | $\geq 1300$ | $\geq 500$ | T1/T5tttt; large $\Delta m(\tilde{g}, \tilde{\chi}_1^0)$ |

reconstructed as a jet and the event can escape the vetoes of Sec. V. Second, if the $W$ boson decays to an electron or muon (including from the decay of a $\tau$ lepton) that is not reconstructed or identified, is not isolated, or lies outside the acceptance of the analysis, the event can escape the vetoes. These two possibilities are referred to as the $\tau_h$ and lost-lepton backgrounds, respectively. They are evaluated, together, using a single-lepton data control sample (CS) collected using the same trigger that is used to collect signal events. The CS events must satisfy the same criteria as the data except for the vetoes of Sec. V, which are replaced by a requirement that there be exactly one isolated electron or muon candidate based on the isolation criteria of Sec. V. To reduce potential contributions from signal processes, CS events must have $m_T < 100$ GeV.

The predicted summed number of $\tau_h$ and lost-lepton events in a search region is given by the number of single-electron or single-muon events in the corresponding region of the CS, multiplied by a translation factor from simulation. Predictions from the single-electron and single-muon samples are determined separately and used as independent constraints in the likelihood fit described in Sec. X. The translation factor is given by the ratio of the summed number of simulated $\tau_h$ and lost-lepton events in the search region to the number of simulated single-electron or single-muon events in the corresponding CS region.

The method is tested using an orthogonal data sample, referred to as the "sideband" (SB), selected using the same criteria as are applied to the data except with $N_t = 0$, $N_b \geq 2$, and $\Delta\phi(\vec{p}_T^{\,miss}, j_{1,2,3,4}) > 0.5$, where the last two requirements reduce contributions from $Z(\nu\bar{\nu}) + $ jets and QCD multijet events. The SB, which is enhanced in events with semileptonic top quark decays, is divided into four intervals of $p_T^{miss}$. The contribution of $\tau_h$ and lost-lepton events to the intervals is determined in an analogous manner to that described above for the search regions, namely by multiplying the number of events in the

corresponding interval of the single-electron or single-muon CS by a translation factor from simulation, defined analogously to the translation factors of the standard analysis. The contributions of $Z + $ jets, QCD multijet, and rare events to the SB are taken directly from simulation. Figure 4 shows the $p_T^{miss}$ distribution in the SB in comparison to the SM prediction. The histogram labeled "$t\bar{t}/t/W$" shows the predicted contribution from $\tau_h$ and lost-lepton events. The total SM prediction is seen to agree with the data within the uncertainties, providing a validation for the translation factor procedure.

Systematic uncertainties in the prediction for the $t\bar{t}$, single top quark, and $W + $ jets background are evaluated from the following sources, based on the uncertainties in the respective quantities: the statistical uncertainty in the translation factors (1–40% depending on the search region), the lepton reconstruction and isolation efficiency (7–43%), the jet and $p_T^{miss}$ energy scale and resolution (up to 64%), the ISR modeling (up to 13%), the PDFs (up to 32%), and the $b$ jet tagging efficiency (1%).

As a cross-check, the lost-lepton background is evaluated using a complementary procedure, described in Ref. [20], based on the single-lepton CS described above and on factors obtained for each search region from $t\bar{t}$, single top quark, and $W + $ jets simulation that account for the acceptance, the isolation efficiency, and the reconstruction-and-identification efficiency. The lost-lepton background evaluated with this approach is consistent with that obtained from the translation factor method.

### B. Background from $Z(\nu\bar{\nu}) + $ jets events

The background from $Z(\nu\bar{\nu}) + $ jets events is evaluated using simulated $Z(\nu\bar{\nu}) + $ jets events that satisfy the search region selection criteria. Two corrections, derived from an event sample enhanced in DY$(Z \to \mu\mu) + $ jets production, are applied to account for differences between data and
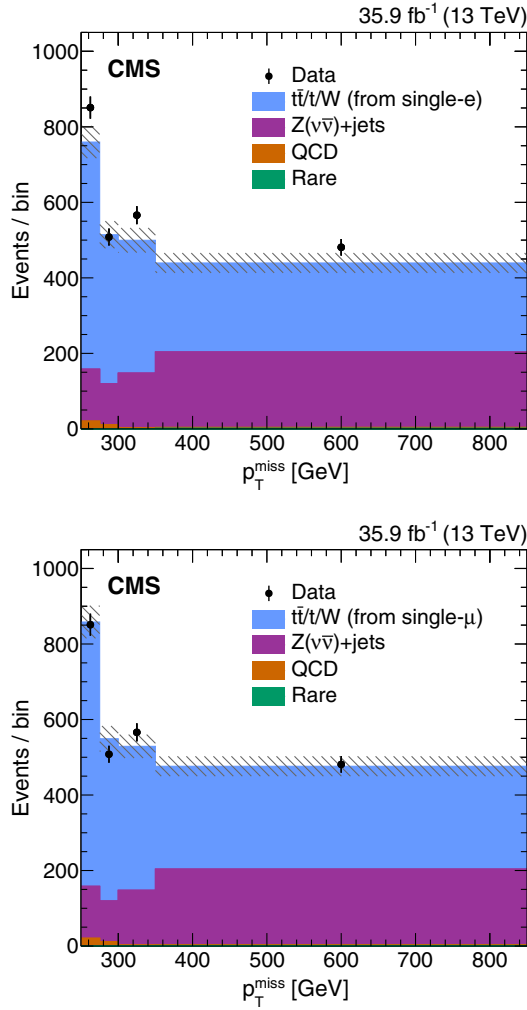
FIG. 4. Distribution of $p_T^{miss}$ in the sideband data sample in comparison to predictions for SM processes. The prediction for $t\bar{t}$, single top quark, and $W + $ jets events is obtained using translation factors applied to a single-electron control sample (top) or to a single-muon control sample (bottom). The hatched bands indicate the statistical uncertainties in the total SM prediction. Note that the data and the predictions for all backgrounds except that for $t\bar{t}$, single top quark, and $W + $ jets events are identical between the left and right plots.

simulation. The trigger to select the DY + jets events requires that there be at least one muon with $p_T > 50$ GeV, while the offline selection requires two oppositely charged muons with a dimuon invariant mass between 81 and 101 GeV, and the highest (second-highest) $p_T$ muon in the event to have $p_T > 50(20)$ GeV. The dimuon system is removed from the events to emulate $\vec{p}_T^{miss}$ in $Z(\nu\bar{\nu}) + $ jets events.

The first correction, which accounts for the $N_j$ distribution, is based on a "loose" dimuon control sample selected by imposing, on the DY-enhanced event sample described in the previous paragraph, the same requirements on $\Delta\phi(\vec{p}_T^{miss}, j_{1,2,3})$, $H_T$, and $N_t$ as are applied to signal

candidate events, but with the less stringent requirement $p_T^{miss} > 100$ GeV and with no requirement on $N_b$. The correction is determined as a function of $N_j$ as the ratio of the number of events in the loose control sample, with non-DY events subtracted using simulation, to the number of events in a similarly selected sample of simulated DY events. The corrections are applied to the $Z(\nu\bar{\nu}) + $ jets simulation as weights based on the value of $N_j$.

The second correction adjusts the overall normalization of the simulated $Z(\nu\bar{\nu}) + $ jets sample. It is derived from a
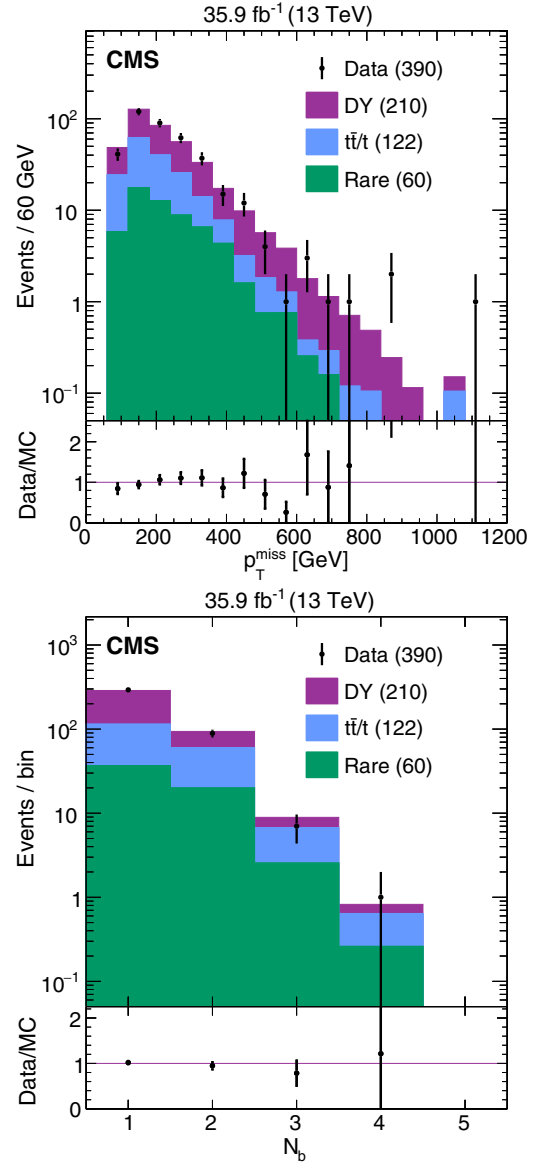


FIG. 5. The $p_T^{miss}$ (top) and $N_b$ (bottom) distributions of data and simulation in the loose dimuon control sample after applying a correction, as described in the text, to account for differences between the data and simulation for the $N_j$ distribution. The lower panels show the ratio between data and simulation. Only statistical uncertainties are shown. The values in parentheses indicate the integrated yields for each component.

"tight" dimuon data control sample selected by applying, to the DY-enhanced event sample described in the first paragraph of this section, the same requirements as are applied to signal events except, of the vetoes described in Sec. V, only the veto on isolated electrons is applied, and there is no requirement on $N_b$. The correction is given by the ratio of the number of events in the tight control sample, with non-DY backgrounds subtracted using simulation, to the number of events in a sample of simulated DY events selected with the same criteria.

Systematic uncertainties in the prediction for the $Z(\nu\bar{\nu})$ + jets background are derived from the shape differences between data and simulation in the loose dimuon control sample as a function of $N_b$, $N_t$, $p_T^{miss}$, $m_{T2}$, and $H_T$ after the first correction described above has been applied. As examples, the post-correction comparisons between data and simulation for the $p_T^{miss}$ and $N_b$ distributions are shown in Fig. 5. The shift in the central value between the data and simulation in the distributions is used to define an additional uncertainty, which varies between 14 and 44% depending on the search region. The statistical uncertainty in the $N_j$ shape correction (1%–46%) and in the overall normalization correction (7.6%) are also taken as systematic uncertainties. Additional systematic uncertainties account for the jet and $p_T^{miss}$ energy scales (1%–71%), the $b$ tagging efficiency (1%–23%), the PDFs and the renormalization and factorization scales (1%–48%), the statistical uncertainty in the simulation (1%–81%, with the results for a few search regions as high as 100%), and the trigger (up to 14%).

### C. Background from multijet events

The background from QCD multijet events is evaluated similarly to the background from $t\bar{t}$, single top quark, and $W$ + jets events. A QCD data control sample is defined using the same trigger and selection criteria as are used to select signal events but with the less restrictive condition $p_T^{miss} > 200$ GeV and with the selection criteria on $\Delta\phi(\vec{p}_T^{miss}, j_{1,2,3})$ inverted. This yields a signal-depleted control sample dominated by QCD multijet events. The predicted number of QCD multijet events in each of the 84 search regions is given by the yield in the corresponding region of the QCD control sample, after contributions from non-QCD SM processes have been subtracted using simulation, multiplied by a translation factor derived from simulated QCD multijet events. The translation factors are applied as a function of $p_T^{miss}$ and $m_{T2}$ for $N_b$ and $N_t \leq 2$, and as a function of $p_T^{miss}$ for $N_b$ or $N_t \geq 3$, and are normalized to data in the $200 < p_T^{miss} < 250$ GeV region of the QCD control sample.

A systematic uncertainty in the QCD multijet prediction for each search region is evaluated as the difference between the event yield obtained directly from the QCD multijet simulation for that region and the prediction obtained by applying the background prediction procedure to simulated QCD multijet samples (30%–500%). Additional sources of uncertainty are from the statistical uncertainty in the translation factors (30%–300%) and the subtraction of the non-QCD-multijet SM contributions to the QCD control sample (2%–50%).
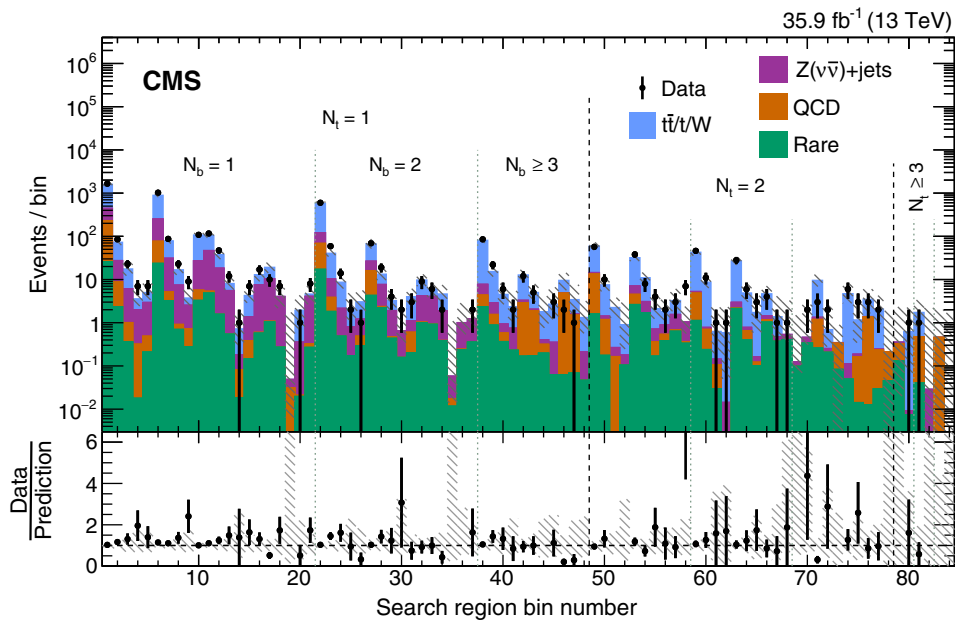


FIG. 6.    Observed event yields (black points) and prefit SM background predictions (filled solid areas) for the 84 search regions, where "prefit" means there is no constraint from the likelihood fit. The lower panel shows the ratio of the data to the total background prediction. The hatched bands correspond to the total uncertainty in the background prediction.

### D. Background from rare processes

Background from rare events forms only a small fraction of the total background and has only a small effect on the final result. Estimates of the rates of rare background processes are taken directly from simulation. The largest component of this background is from $t\bar{t}Z$ production. To validate the $t\bar{t}Z$ cross section in the simulation, a three-lepton control sample is selected. The yields of events in this sample between simulation and data are found to agree within the statistical uncertainty of 30%, which is taken as the systematic uncertainty in the $t\bar{t}Z$ background estimate.

## X. RESULTS AND INTERPRETATION

The number of observed events and the predicted number of SM background events in each of the 84 search regions are summarized in Fig. 6. Numerical values are given in Tables II–IV of Appendix. The corresponding results for the aggregate search regions are presented in Fig. 7, with numerical values in Table V of Appendix. No statistically significant deviation between the data and the background predictions is observed. The largest source of background typically arises from $t\bar{t}$ or $W$ + jets production, followed by $Z(\nu\bar{\nu})$ + jets production. The latter background source can be dominant, however, in search regions with a high $p_T^{miss}$ threshold. The contributions of the QCD multijet and rare backgrounds are small in all regions.

Exclusion limits are derived for the signal models of Sec. II using a binned likelihood fit to the data. The likelihood function is given by the product of Poisson probability density functions, one for each search region and for each of
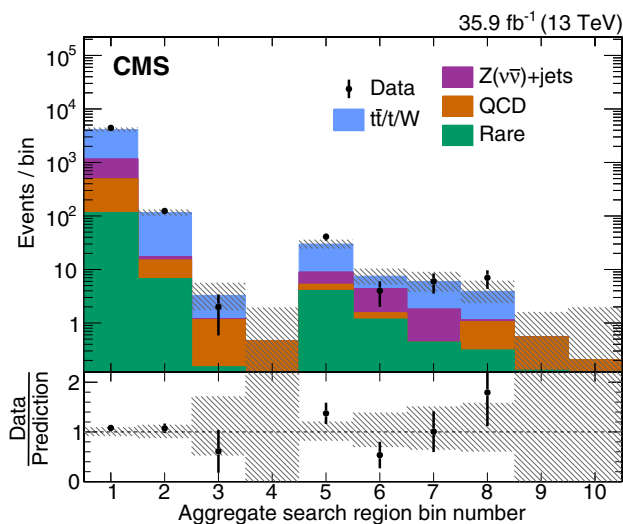
the corresponding regions of the single-electron, single-muon, and QCD data control samples, that account for the background predictions and signal yields. The uncertainties are treated as nuisance parameters with log-normal probability density functions. Correlations between search regions are taken into account. Upper limits at 95% confidence level (CL) on the SUSY production cross sections are calculated using a modified frequentist approach with the $CL_s$ criterion [73,74] and asymptotic results for the test statistic [75,76]. Signal models for which the 95% CL upper limit on the production cross section falls below the theoretical cross section (based on NLO + NLL calculations [55]) are considered to be excluded by the analysis.

The uncertainties in the signal modeling are determined individually for each search region and account for the following sources: the statistical uncertainty in the simulated event samples, the integrated luminosity (2.5% [77]), the lepton and isolated-track veto efficiencies (up to 6.8%), the $b$ tagging efficiency (up to 21%), the trigger efficiency (up to 2.6%), the renormalization and factorization scales (up to 3.5%), the ISR modeling (up to 46%), the jet energy scale corrections (up to 34%), the top quark reconstruction efficiency (up to 14%), and the modeling of the fast simulation compared with the full simulation for top quark
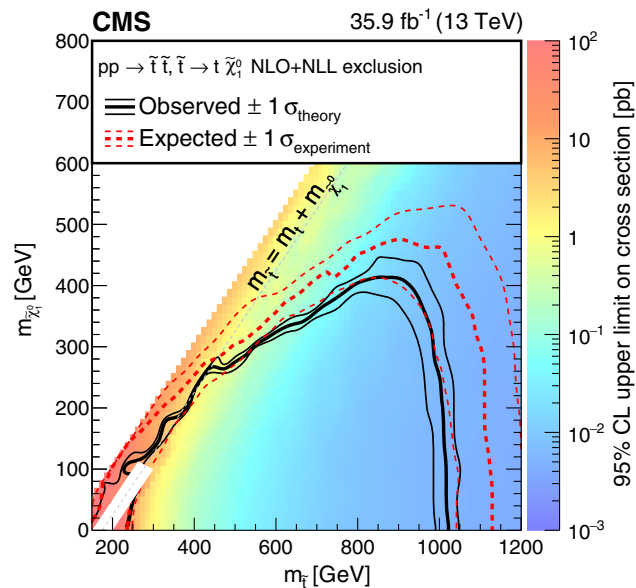


FIG. 8. The 95% CL upper limit on the production cross section of the T2tt simplified model as a function of the top squark and LSP masses. The solid black curves represent the observed exclusion contour with respect to NLO + NLL signal cross sections and the change in this contour due to variation of these cross sections within their theoretical uncertainties [55]. The dashed red curves indicate the mean expected exclusion contour and the region containing 68% of the distribution of expected exclusion limits under the background-only hypothesis. No interpretation is provided for signal models for which $|m_{\tilde{t}} - m_{\tilde{\chi}_1^0} - m_t| \le 25$ GeV and $m_{\tilde{t}} \le 275$ GeV because signal events are essentially indistinguishable from SM $t\bar{t}$ events in this region, rendering the signal event acceptance difficult to model.



FIG. 7. Observed event yields (black points) and prefit SM background predictions (filled solid areas) for the 10 aggregate search regions, where "prefit" means there is no constraint from the likelihood fit. The lower panel shows the ratio of the data to the total background prediction. The hatched bands correspond to the total uncertainty in the background prediction.

reconstruction and mistagging (up to 24%). All uncertainties except those from the statistical precision of the simulation are treated as fully correlated between search regions. Signal contamination, namely potential contributions of signal events to the control samples, is taken into account when computing the limits. Note that signal contamination is significant only for the single-lepton control samples of Sec. IX A and is negligible for the dimuon and inverted-$\Delta\phi$ control samples of Secs. IX B and IX C.

Figure 8 shows the 95% CL exclusion limits obtained for the T2tt model of direct top squark pair production:

top squark masses up to 1020 GeV and LSP masses up to 430 GeV are excluded. The results for the four models of gluino pair production, T1tttt, T1ttbb, T5tttt, and T5ttcc, are shown in Fig. 9. Gluino masses up to 2040 GeV and LSP masses up to 1150 GeV are excluded for the T1tttt model, with corresponding limits of 2020 and 1150 GeV for the T1ttbb model, 2020 and 1150 GeV for the T5tttt model, and 1810 and 1100 GeV for the T5ttcc model. The limits on the gluino mass are somewhat lower for the T1ttbb model than for the T1tttt model because of the smaller average number of top quarks. The lower limit



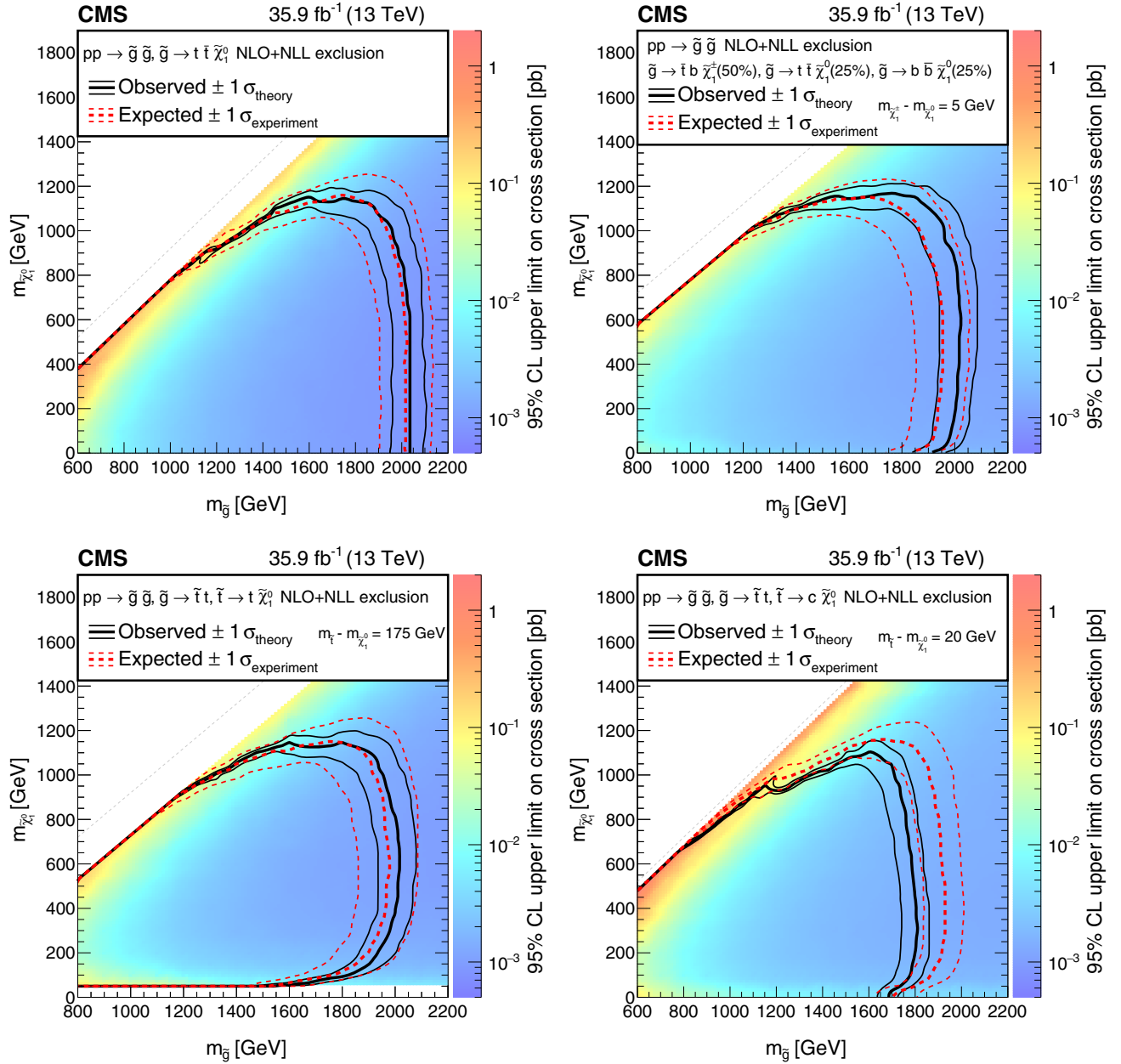FIG. 9. The 95% CL upper limit on the production cross section of the T1tttt (upper left), T1ttbb (upper right), T5tttt (bottom left), and T5ttcc (bottom right) simplified models as a function of the gluino and LSP masses. The meaning of the curves is explained in the Fig. 8 caption. Limits are not given for the T5tttt model for $m_{\tilde{\chi}_1^0} < 50$ GeV for the reason stated in the text.

of up to 2040 GeV obtained for the gluino mass in the T1tttt model improves the corresponding limits of Refs. [17,18] by around 100 GeV, while the limit on the gluino mass of up to 1810 GeV obtained for the T5ttcc model improves that presented in Ref. [78] by 560 GeV. This emphasizes the effectiveness of top quark tagging in all-hadronic events as a means to search for new physics that yields top quarks, and the complementarity of our study with respect to searches based on other signatures.

In the case of the T5tttt model there is a significant degradation of the exclusion limit as $m_{\tilde{\chi}_1^0}$ approaches zero. This is a consequence of the kinematics of the $\tilde{t} \to t\tilde{\chi}_1^0$ decay, by which only a small portion of the top squark momentum is transferred to the LSP if the LSP is lighter than the top quark. The events then have very small $p_T^{miss}$ and a small selection efficiency. The correction to account for signal contamination becomes larger than the number of selected signal events and the statistical treatment to account for signal contamination becomes unreliable. For this reason, we do not present results for the T5tttt model if $m_{\tilde{\chi}_1^0} < 50$ GeV.

## XI. SUMMARY

Results are presented from a search for direct and gluino-mediated top squark production in proton-proton collisions at a center-of-mass energy of 13 TeV. The centerpiece of the analysis is a top quark tagging algorithm that identifies hadronically decaying top quarks with high efficiency across a wide range of top quark transverse momentum $p_T$. The search is based on all-hadronic events with at least four jets, at least one tagged top quark, at least one tagged bottom quark jet, and a large imbalance in transverse momentum $p_T^{miss}$. The data correspond to an integrated luminosity of 35.9 fb$^{-1}$ collected with the CMS detector at the LHC in 2016. A set of 84 search regions is defined based on $p_T^{miss}$, the mass variable $m_{T2}$, the scalar $p_T$ sum of jets $H_T$, the number of tagged top quarks, and the number of tagged bottom quark jets. No statistically significant excess of events is observed relative to the expectation from the standard model.

Cross section upper limits at 95% confidence level are evaluated for a simplified model of direct top squark pair production, in which the top squarks decay to a top quark and the lightest supersymmetric particle (LSP) neutralino, and for simplified models of gluino pair production, in which the gluinos decay to final states containing top quarks and LSPs. Using the signal cross sections calculated with next-to-leading-order plus next-to-leading-logarithm accuracy, 95% confidence level lower limits are set on the masses of the top squark, the gluino, and the LSP. For the model of direct top squark pair production, top squark masses up to 1020 GeV and LSP masses up to 430 GeV are excluded. For the models of gluino pair production, gluinos with masses as large as 1810 to 2040 GeV are excluded,

depending on the model, with corresponding exclusions for LSPs with masses as large as 1100 to 1150 GeV. These results significantly extend those of our previous study [20]. The use of top quark tagging provides a novel means to search for new phenomena at the LHC, yielding complementary sensitivity to other approaches.

## APPENDIX: PREFIT BACKGROUND PREDICTIONS

Tables II–IV present the prefit predictions for the number of standard model background events in each of the 84 search regions, along with the number of observed events. "Prefit" means that there is no constraint from the likelihood fit. The corresponding information for the 10 aggregate search regions is presented in Table V.

TABLE II.   The observed number of events and the total background prediction for search regions with $N_t = 1$ and $N_b = 1$. The first uncertainty in the background prediction is statistical and the second is systematic.

| Search region | $N_t$ | $N_b$ | $m_{T2}$ [GeV] | $p_T^{miss}$ [GeV] | Data | Predicted background |
|---|---|---|---|---|---|---|
| 1 | 1 | 1 | 200–300 | 250–400 | 1649 | $1600 \pm 30^{+130}_{-140}$ |
| 2 | 1 | 1 | 200–300 | 400–500 | 85 | $73^{+7}_{-6}{}^{+12}_{-9}$ |
| 3 | 1 | 1 | 200–300 | 500–600 | 23 | $18^{+4}_{-3}{}^{+6}_{-4}$ |
| 4 | 1 | 1 | 200–300 | 600–750 | 7 | $3.6^{+1.9}_{-0.8}{}^{+1.9}_{-0.8}$ |
| 5 | 1 | 1 | 200–550 | ≥750 | 7 | $5.0^{+2.4}_{-1.1}{}^{+1.9}_{-1.2}$ |
| 6 | 1 | 1 | 300–400 | 250–400 | 1020 | $890 \pm 20^{+80}_{-80}$ |
| 7 | 1 | 1 | 300–400 | 400–500 | 87 | $79^{+7}_{-6} \pm 9$ |
| 8 | 1 | 1 | 300–400 | 500–600 | 23 | $17^{+4}_{-2} \pm 3$ |
| 9 | 1 | 1 | 300–400 | 600–750 | 9 | $3.7^{+2.2}_{-0.8}{}^{+1.6}_{-0.9}$ |
| 10 | 1 | 1 | 400–550 | 250–400 | 108 | $107^{+8}_{-7} \pm 10$ |
| 11 | 1 | 1 | 400–550 | 400–500 | 116 | $105^{+7}_{-6} \pm 10$ |
| 12 | 1 | 1 | 400–550 | 500–600 | 47 | $38^{+5}_{-4} \pm 7$ |
| 13 | 1 | 1 | 400–550 | 600–750 | 12 | $8.1^{+2.4}_{-1.2} \pm 1.9$ |
| 14 | 1 | 1 | 550–750 | 250–400 | 1 | $0.7^{+1.0}_{-0.3}{}^{+0.4}_{-0.2}$ |
| 15 | 1 | 1 | 550–750 | 400–500 | 7 | $4.3^{+2.0}_{-1.1} \pm 0.8$ |
| 16 | 1 | 1 | 550–750 | 500–600 | 17 | $13^{+3}_{-2} \pm 3$ |
| 17 | 1 | 1 | 550–750 | 600–750 | 10 | $19^{+3}_{-2} \pm 4$ |
| 18 | 1 | 1 | 550–750 | ≥750 | 7 | $4.0^{+1.5}_{-0.3} \pm 1.8$ |
| 19 | 1 | 1 | ≥750 | 250–600 | 0 | $0.1^{+1.7}_{-0.1} \pm 0.1$ |
| 20 | 1 | 1 | ≥750 | 600–750 | 1 | $1.9^{+2.2}_{-1.0}{}^{+0.9}_{-0.8}$ |
| 21 | 1 | 1 | ≥750 | ≥750 | 8 | $4.6^{+1.6}_{-0.5} \pm 1.9$ |

TABLE III. The observed number of events and the total background prediction for search regions with $N_t = 1$ and $N_b \geq 2$. The first uncertainty in the background prediction is statistical and the second is systematic.

| Search region | $N_t$ | $N_b$ | $m_{T2}$ [GeV] | $p_T^{miss}$ [GeV] | Data | Predicted background |
|---|---|---|---|---|---|---|
| 22 | 1 | 2 | 200–350 | 250–400 | 596 | $580 \pm 20 \pm 60$ |
| 23 | 1 | 2 | 200–350 | 400–500 | 59 | $41^{+6}_{-5}{}^{+6}_{-5}$ |
| 24 | 1 | 2 | 200–350 | 500–600 | 14 | $8.7^{+3.4}_{-2.1} \pm 1.3$ |
| 25 | 1 | 2 | 200–350 | 600–750 | 2 | $2.1^{+2.7}_{-0.8} \pm 0.5$ |
| 26 | 1 | 2 | 200–650 | $\geq 750$ | 1 | $3.0^{+2.4}_{-1.0}{}^{+0.9}_{-0.6}$ |
| 27 | 1 | 2 | 350–450 | 250–400 | 69 | $67^{+6}_{-5}{}^{+18}_{-14}$ |
| 28 | 1 | 2 | 350–450 | 400–500 | 19 | $13^{+4}_{-2} \pm 3$ |
| 29 | 1 | 2 | 350–450 | 500–600 | 4 | $3.2^{+2.1}_{-0.9} \pm 1.0$ |
| 30 | 1 | 2 | 350–450 | 600–750 | 2 | $0.6^{+1.4}_{-0.1} \pm 0.3$ |
| 31 | 1 | 2 | 450–650 | 250–400 | 3 | $4.0^{+2.0}_{-1.1}{}^{+0.7}_{-0.9}$ |
| 32 | 1 | 2 | 450–650 | 400–500 | 9 | $9.7^{+2.7}_{-1.8}{}^{+2.1}_{-2.0}$ |
| 33 | 1 | 2 | 450–650 | 500–600 | 6 | $6.0^{+1.6}_{-0.9} \pm 1.9$ |
| 34 | 1 | 2 | 450–650 | 600–750 | 2 | $4.6^{+2.6}_{-1.3} \pm 1.2$ |
| 35 | 1 | 2 | $\geq 650$ | 250–600 | 0 | $0.06^{+1.03}_{-0.03} \pm 0.03$ |
| 36 | 1 | 2 | $\geq 650$ | 600–750 | 0 | $1.0^{+1.8}_{-0.1} \pm 0.5$ |
| 37 | 1 | 2 | $\geq 650$ | $\geq 750$ | 2 | $1.2^{+1.1}_{-0.1} \pm 0.5$ |
| 38 | 1 | $\geq 3$ | 300–1000 | 250–350 | 85 | $81^{+9}_{-8} \pm 7$ |
| 39 | 1 | $\geq 3$ | 300–1000 | 350–450 | 22 | $15^{+5}_{-3} \pm 2$ |
| 40 | 1 | $\geq 3$ | 300–1000 | 450–550 | 6 | $4.5^{+3.4}_{-1.7} \pm 0.8$ |
| 41 | 1 | $\geq 3$ | 300–1000 | $\geq 550$ | 2 | $2.4^{+2.9}_{-1.0}{}^{+1.0}_{-0.7}$ |
| 42 | 1 | $\geq 3$ | 1000–1500 | 250–350 | 12 | $13^{+4}_{-3} \pm 2$ |
| 43 | 1 | $\geq 3$ | 1000–1500 | 350–450 | 5 | $5.0^{+2.7}_{-1.7} \pm 1.1$ |
| 44 | 1 | $\geq 3$ | 1000–1500 | 450–550 | 0 | $1.8^{+2.3}_{-1.0} \pm 0.4$ |
| 45 | 1 | $\geq 3$ | 1000–1500 | $\geq 550$ | 3 | $2.7^{+3.9}_{-1.4}{}^{+0.6}_{-0.5}$ |
| 46 | 1 | $\geq 3$ | $\geq 1500$ | 250–350 | 2 | $9.6^{+3.4}_{-2.2} \pm 3.3$ |
| 47 | 1 | $\geq 3$ | $\geq 1500$ | 350–550 | 1 | $3.4^{+2.3}_{-1.2}{}^{+3.4}_{-1.5}$ |
| 48 | 1 | $\geq 3$ | $\geq 1500$ | $\geq 550$ | 0 | $1.3^{+1.8}_{-0.7} \pm 0.3$ |

TABLE IV. The observed number of events and the total background prediction for search regions with $N_t \geq 2$. The first uncertainty in the background prediction is statistical and the second is systematic.

| Search region | $N_t$ | $N_b$ | $m_{T2}$ [GeV] | $p_T^{miss}$ [GeV] | Data | Predicted background |
|---|---|---|---|---|---|---|
| 49 | 2 | 1 | 200–300 | 250–350 | 57 | $60^{+6}_{-5} \pm 11$ |
| 50 | 2 | 1 | 200–300 | 350–450 | 10 | $7.5^{+2.5}_{-1.7}{}^{+1.8}_{-1.4}$ |
| 51 | 2 | 1 | 200–300 | 450–600 | 0 | $2.2^{+1.4}_{-0.8}{}^{+0.8}_{-0.5}$ |
| 52 | 2 | 1 | 200–450 | $\geq 600$ | 0 | $0.9^{+2.0}_{-0.6}{}^{+0.4}_{-0.3}$ |
| 53 | 2 | 1 | 300–450 | 250–350 | 38 | $32^{+5}_{-4} \pm 3$ |
| 54 | 2 | 1 | 300–450 | 350–450 | 8 | $11^{+3}_{-2} \pm 2$ |
| 55 | 2 | 1 | 300–450 | 450–600 | 4 | $2.1^{+1.7}_{-0.7}{}^{+0.8}_{-0.5}$ |
| 56 | 2 | 1 | $\geq 450$ | 250–450 | 2 | $1.8^{+1.5}_{-0.6} \pm 0.4$ |
| 57 | 2 | 1 | $\geq 450$ | 450–600 | 3 | $3.3^{+2.7}_{-1.1} \pm 0.9$ |
| 58 | 2 | 1 | $\geq 450$ | $\geq 600$ | 7 | $1.0^{+1.2}_{-0.1} \pm 0.5$ |
| 59 | 2 | 2 | 200–300 | 250–350 | 46 | $43 \pm 5^{+5}_{-6}$ |

*(Table continued)*

TABLE IV. *(Continued)*

| Search region | $N_t$ | $N_b$ | $m_{T2}$ [GeV] | $p_T^{miss}$ [GeV] | Data | Predicted background |
|---|---|---|---|---|---|---|
| 60 | 2 | 2 | 200–300 | 350–450 | 11 | $8.7^{+2.7}_{-1.9}{}^{+1.4}_{-1.3}$ |
| 61 | 2 | 2 | 200–300 | 450–600 | 1 | $0.6^{+1.6}_{-0.4}{}^{+0.3}_{-0.2}$ |
| 62 | 2 | 2 | 200–400 | ≥600 | 1 | $0.6^{+1.7}_{-0.5}\pm0.2$ |
| 63 | 2 | 2 | 300–400 | 250–350 | 28 | $27^{+5}_{-4}\pm3$ |
| 64 | 2 | 2 | 300–400 | 350–450 | 6 | $4.9^{+2.9}_{-1.6}\pm0.9$ |
| 65 | 2 | 2 | 300–400 | 450–600 | 3 | $1.7^{+2.4}_{-1.0}{}^{+0.6}_{-0.5}$ |
| 66 | 2 | 2 | 400–500 | 250–450 | 4 | $4.7^{+2.3}_{-1.2}{}^{+0.7}_{-0.8}$ |
| 67 | 2 | 2 | 400–500 | 450–600 | 1 | $1.4^{+2.7}_{-0.7}{}^{+0.4}_{-0.6}$ |
| 68 | 2 | 2 | ≥400 | ≥600 | 1 | $0.5^{+2.7}_{-0.1}\pm0.2$ |
| 69 | 2 | 2 | ≥500 | 250–450 | 0 | $0.1^{+1.4}_{-0.1}\pm0.1$ |
| 70 | 2 | 2 | ≥500 | 450–600 | 2 | $0.5^{+2.2}_{-0.1}\pm0.1$ |
| 71 | 2 | ≥3 | 300–900 | 250–350 | 3 | $9.6^{+3.0}_{-2.1}\pm1.7$ |
| 72 | 2 | ≥3 | 300–900 | 350–500 | 2 | $0.7^{+2.0}_{-0.4}\pm0.2$ |
| 73 | 2 | ≥3 | 300–1300 | ≥500 | 0 | $0.3^{+0.5}_{-0.3}{}^{+0.3}_{-0.2}$ |
| 74 | 2 | ≥3 | 900–1300 | 250–350 | 6 | $4.7^{+2.9}_{-1.7}{}^{+0.7}_{-0.9}$ |
| 75 | 2 | ≥3 | 900–1300 | 350–500 | 3 | $1.2^{+1.6}_{-0.7}\pm0.4$ |
| 76 | 2 | ≥3 | ≥1300 | 250–350 | 3 | $3.5^{+2.1}_{-1.2}\pm1.4$ |
| 77 | 2 | ≥3 | ≥1300 | 350–500 | 2 | $2.1^{+2.1}_{-1.0}{}^{+0.4}_{-0.5}$ |
| 78 | 2 | ≥3 | ≥1300 | ≥500 | 0 | $0.2^{+1.7}_{-0.3}\pm0.2$ |
| 79 | ≥3 | 1 | ≥300 | 250–350 | 0 | $0.3^{+2.0}_{-0.3}\pm0.2$ |
| 80 | ≥3 | 1 | ≥300 | ≥350 | 1 | $0.6^{+1.6}_{-0.5}\pm0.2$ |
| 81 | ≥3 | 2 | ≥300 | 250–400 | 1 | $1.7^{+1.5}_{-0.7}{}^{+0.6}_{-0.5}$ |
| 82 | ≥3 | 2 | ≥300 | ≥400 | 0 | $0.1^{+2.2}_{-0.1}\pm0.1$ |
| 83 | ≥3 | ≥3 | ≥300 | 250–350 | 0 | $0.5^{+1.5}_{-0.4}\pm0.5$ |
| 84 | ≥3 | ≥3 | ≥ 300 | ≥350 | 0 | $0.0^{+1.6}_{-0.0}{}^{+0.1}_{-0.0}$ |

TABLE V. The observed number of events and the total background prediction for the aggregate search regions. The first uncertainty in the background prediction is statistical and the second is systematic.

| Search region | $N_t$ | $N_b$ | $m_{T2}$ [GeV] | $p_T^{miss}$ [GeV] | Data | Predicted background |
|---|---|---|---|---|---|---|
| 1 | ≥1 | ≥1 | ≥200 | ≥250 | 4424 | $4100\pm50^{+390}_{-340}$ |
| 2 | ≥2 | ≥2 | ≥200 | ≥250 | 124 | $116\pm8^{+15}_{-12}$ |
| 3 | ≥3 | ≥1 | ≥200 | ≥250 | 2 | $3.3^{+2.0}_{-1.1}{}^{+1.2}_{-1.1}$ |
| 4 | ≥3 | ≥3 | ≥200 | ≥250 | 0 | $0.5^{+1.4}_{-0.4}\pm0.5$ |
| 5 | ≥2 | ≥1 | ≥200 | ≥400 | 41 | $30^{+4}_{-3}{}^{+5}_{-4}$ |
| 6 | ≥1 | ≥2 | ≥600 | ≥400 | 4 | $7.5^{+2.1}_{-1.2}{}^{+2.0}_{-1.9}$ |

| Search region | $N_t$ | $N_b$ | $H_T$ [GeV] | $p_T^{miss}$ [GeV] | Data | Predicted background |
|---|---|---|---|---|---|---|
| 7 | ≥1 | ≥2 | ≥1400 | ≥500 | 6 | $6.0^{+2.7}_{-1.5}\pm1.5$ |
| 8 | ≥2 | ≥3 | ≥600 | ≥350 | 7 | $3.9^{+2.1}_{-1.2}\pm0.9$ |
| 9 | ≥2 | ≥3 | ≥300 | ≥500 | 0 | $0.6^{+1.0}_{-0.4}\pm0.4$ |
| 10 | ≥2 | ≥3 | ≥1300 | ≥500 | 0 | $0.2^{+1.8}_{-0.3}\pm0.2$ |

[1] ATLAS Collaboration, Observation of a new particle in the search for the Standard Model Higgs boson with the ATLAS detector at the LHC, Phys. Lett. B **716**, 1 (2012).

[2] CMS Collaboration, Observation of a new boson at a mass of 125 GeV with the CMS experiment at the LHC, Phys. Lett. B **716**, 30 (2012).

[3] CMS Collaboration, Observation of a new boson with mass near 125 GeV in pp collisions at $\sqrt{s} = 7$ and 8 TeV, J. High Energy Phys. 06 (2013) 081.

[4] ATLAS and CMS Collaborations, Combined Measurement of the Higgs Boson Mass in pp Collisions at $\sqrt{s} = 7$ and 8 TeV with the ATLAS and CMS Experiments, Phys. Rev. Lett. **114**, 191803 (2015).

[5] R. Barbieri and G. F. Giudice, Upper bounds on supersymmetric particle masses, Nucl. Phys. **B306**, 63 (1988).

[6] P. Ramond, Dual theory for free fermions, Phys. Rev. D **3**, 2415 (1971).

[7] Yu. A. Gol'fand and E. P. Likhtman, Extension of the algebra of Poincaré group generators and violation of P invariance, JETP Lett. **13**, 323 (1971).

[8] D. V. Volkov and V. P. Akulov, Possible universal neutrino interaction, JETP Lett. **16**, 438 (1972).

[9] J. Wess and B. Zumino, Supergauge transformations in four-dimensions, Nucl. Phys. **B70**, 39 (1974).

[10] P. Fayet, Supergauge invariant extension of the Higgs mechanism and a model for the electron and its neutrino, Nucl. Phys. **B90**, 104 (1975).

[11] R. Barbieri, S. Ferrara, and C. A. Savoy, Gauge models with spontaneously broken local supersymmetry, Phys. Lett. B **119**, 343 (1982).

[12] A. H. Chamseddine, R. L. Arnowitt, and P. Nath, Locally Supersymmetric Grand Unification, Phys. Rev. Lett. **49**, 970 (1982).

[13] L. J. Hall, J. D. Lykken, and S. Weinberg, Supergravity as the messenger of supersymmetry breaking, Phys. Rev. D **27**, 2359 (1983).

[14] G. L. Kane, C. F. Kolda, L. Roszkowski, and J. D. Wells, Study of constrained minimal supersymmetry, Phys. Rev. D **49**, 6173 (1994).

[15] M. Papucci, J. T. Ruderman, and A. Weiler, Natural SUSY endures, J. High Energy Phys. 09 (2012) 035.

[16] ATLAS Collaboration, Search for a scalar partner of the top quark in the jets plus missing transverse momentum final state at $\sqrt{s} = 13$ TeV with the ATLAS detector, arXiv:1709.04183.

[17] CMS Collaboration, Search for supersymmetry in multijet events with missing transverse momentum in proton-proton collisions at 13 TeV, Phys. Rev. D **96**, 032003 (2017).

[18] CMS Collaboration, Search for new phenomena with the $M_{T2}$ variable in the all-hadronic final state produced in proton-proton collisions at $\sqrt{s} = 13$ TeV, Eur. Phys. J. C **77**, 710 (2017).

[19] CMS Collaboration, Search for direct production of supersymmetric partners of the top quark in the all-jets final state in proton-proton collisions at $\sqrt{s} = 13$ TeV, J. High Energy Phys. 10 (2017) 005.

[20] CMS Collaboration, Search for supersymmetry in the all-hadronic final state using top quark tagging in pp collisions at $\sqrt{s} = 13$ TeV, Phys. Rev. D **96**, 012004 (2017).

[21] C. G. Lester and D. J. Summers, Measuring masses of semi-invisibly decaying particles pair produced at hadron colliders, Phys. Lett. B **463**, 99 (1999).

[22] A. Barr, C. Lester, and P. Stephens, A variable for measuring masses at hadron colliders when missing energy is expected; $m_{T2}$: The truth behind the glamour, J. Phys. G **29**, 2343 (2003).

[23] J. Alwall, P. Schuster, and N. Toro, Simplified models for a first characterization of new physics at the LHC, Phys. Rev. D **79**, 075020 (2009).

[24] J. Alwall, M.-P. Le, M. Lisanti, and J. G. Wacker, Model-independent jets plus missing energy searches, Phys. Rev. D **79**, 015005 (2009).

[25] D. Alves et al. (LHC New Physics Working Group), Simplified models for LHC new physics searches, J. Phys. G **39**, 105005 (2012).

[26] D. Alves, E. Izaguirre, and J. G. Wacker, Where the side-walk ends: Jets and missing energy search strategies for the 7 TeV LHC, J. High Energy Phys. 10 (2011) 012.

[27] CMS Collaboration, Interpretation of searches for super-symmetry with simplified models, Phys. Rev. D **88**, 052017 (2013).

[28] CMS Collaboration, The CMS experiment at the CERN LHC, J. Instrum. **3**, S08004 (2008).

[29] CMS Collaboration, The CMS trigger system, J. Instrum. **12**, P01020 (2017).

[30] CMS Collaboration, Particle-flow reconstruction and global event description with the CMS detector, J. Instrum. **12**, P10003 (2017).

[31] CMS Collaboration, Performance of electron reconstruction and selection with the CMS detector in proton-proton collisions at $\sqrt{s} = 8$ TeV, J. Instrum. **10**, P06005 (2015).

[32] CMS Collaboration, The performance of the CMS muon detector in proton-proton collisions at $\sqrt{s} = 7$ TeV at the LHC, J. Instrum. **8**, P11002 (2013).

[33] M. Cacciari, G. P. Salam, and G. Soyez, The anti-$k_t$ jet clustering algorithm, J. High Energy Phys. 04 (2008) 063.

[34] CMS Collaboration, CMS Physics Analysis Summary No. CMS-PAS-JME-10-003, 2010, http://cds.cern.ch/record/1279362.

[35] M. Cacciari and G. P. Salam, Pileup subtraction using jet areas, Phys. Lett. B **659**, 119 (2008).

[36] M. Cacciari, G. P. Salam, and G. Soyez, FastJet user manual, Eur. Phys. J. C **72**, 1896 (2012).

[37] CMS Collaboration, Jet energy scale and resolution in the CMS experiment in pp collisions at 8 TeV, J. Instrum. **12**, P02014 (2017).

[38] CMS Collaboration, CMS Physics Analysis Summary No. CMS-PAS-BTV-15-001, 2016, https://cds.cern.ch/record/2138504.

[39] CMS Collaboration, Identification of b-quark jets with the CMS experiment, J. Instrum. **8**, P04013 (2013).

[40] D. Bertolini, P. Harris, M. Low, and N. Tran, Pileup per particle identification, J. High Energy Phys. 10 (2014) 059.

[41] CMS Collaboration (CMS), CMS Physics Analysis Summary No. CMS-PAS-JME-14-001, 2014, https://cds.cern.ch/record/2138504.

[42] G. Arnison et al. (UA1 Collaboration), Experimental observation of isolated large transverse energy electrons with associated missing energy at $\sqrt{s} = 540$ GeV, Phys. Lett. **122B**, 103 (1983).

[43] J. Alwall, R. Frederix, S. Frixione, V. Hirschi, F. Maltoni, O. Mattelaer, H. S. Shao, T. Stelzer, P. Torrielli, and M. Zaro, The automated computation of tree-level and next-to-leading order differential cross sections, and their matching to parton shower simulations, J. High Energy Phys. 07 (2014) 079.

[44] J. Alwall *et al.*, Comparative study of various algorithms for the merging of parton showers and matrix elements in hadronic collisions, Eur. Phys. J. C **53**, 473 (2008).

[45] R. D. Ball *et al.* (NNPDF Collaboration), Parton distributions for the LHC Run II, J. High Energy Phys. 04 (2015) 040.

[46] P. Nason, A new method for combining NLO QCD with shower Monte Carlo algorithms, J. High Energy Phys. 11 (2004) 040.

[47] S. Frixione, P. Nason, and C. Oleari, Matching NLO QCD computations with Parton Shower simulations: The POW-HEG method, J. High Energy Phys. 11 (2007) 070.

[48] S. Alioli, P. Nason, C. Oleari, and E. Re, A general framework for implementing NLO calculations in shower Monte Carlo programs: The POWHEG BOX, J. High Energy Phys. 06 (2010) 043.

[49] E. Re, Single-top *Wt*-channel production matched with parton showers using the POWHEG method, Eur. Phys. J. C **71**, 1547 (2011).

[50] R. Frederix and S. Frixione, Merging meets matching in MC@NLO, J. High Energy Phys. 12 (2012) 061.

[51] T. Sjöstrand, S. Mrenna, and P. Z. Skands, A brief introduction to PYTHIA 8.1, Comput. Phys. Commun. **178**, 852 (2008).

[52] CMS Collaboration, Event generator tunes obtained from underlying event and multiparton scattering measurements, Eur. Phys. J. C **76**, 155 (2016).

[53] S. Agostinelli *et al.* (GEANT4 Collaboration), GEANT4—a simulation toolkit, Nucl. Instrum. Methods Phys. Res., Sect. A **506**, 250 (2003).

[54] S. Abdullin, P. Azzi, F. Beaudette, P. Janot, and A. Perrotta, The fast simulation of the CMS detector at LHC, J. Phys. Conf. Ser. **331**, 032049 (2011).

[55] C. Borschensky, M. Krämer, A. Kulesza, M. Mangano, S. Padhi, T. Plehn, and X. Portell, Squark and gluino production cross sections in pp collisions at $\sqrt{s} = 13$, 14, 33 and 100 TeV, Eur. Phys. J. C **74**, 3174 (2014).

[56] M. Czakon and A. Mitov, Top++: A program for the calculation of the top-pair cross-section at hadron colliders, Comput. Phys. Commun. **185**, 2930 (2014).

[57] P. Kant, O. M. Kind, T. Kintscher, T. Lohse, T. Martini, S. Mölbitz, P. Rieck, and P. Uwer, HATHOR for single top-quark production: Updated predictions and uncertainty estimates for single top-quark production in hadronic collisions, Comput. Phys. Commun. **191**, 74 (2015).

[58] M. Aliev, H. Lacker, U. Langenfeld, S. Moch, P. Uwer, and M. Wiedermann, HATHOR—Hadronic Top and Heavy quarks cross section calculator, Comput. Phys. Commun. **182**, 1034 (2011).

[59] T. Gehrmann, M. Grazzini, S. Kallweit, P. Maierhöfer, A. von Manteuffel, S. Pozzorini, D. Rathlev, and L. Tancredi, $W^+W^-$ Production at Hadron Colliders in Next to Next to Leading Order QCD, Phys. Rev. Lett. **113**, 212001 (2014).

[60] J. M. Campbell and R. K. Ellis, An update on vector boson pair production at hadron colliders, Phys. Rev. D **60**, 113006 (1999).

[61] J. M. Campbell, R. Keith Ellis, and C. Williams, Vector boson pair production at the LHC, J. High Energy Phys. 07 (2011) 018.

[62] Y. Li and F. Petriello, Combining QCD and electroweak corrections to dilepton production in FEWZ, Phys. Rev. D **86**, 094034 (2012).

[63] CMS Collaboration, CMS Physics Analysis Summary No. CMS-PAS-JME-15-002, 2016, https://cds.cern.ch/record/2126325.

[64] ATLAS Collaboration, Identification of high transverse momentum top quarks in pp collisions at $\sqrt{s} = 8$ TeV with the ATLAS detector, J. High Energy Phys. 06 (2016) 093.

[65] M. Dasgupta, A. Fregoso, S. Marzani, and G. P. Salam, Towards an understanding of jet substructure, J. High Energy Phys. 09 (2013) 029.

[66] A. J. Larkoski, S. Marzani, G. Soyez, and J. Thaler, Soft drop, J. High Energy Phys. 05 (2014) 146.

[67] CMS Collaboration (CMS), CMS Physics Analysis Summary No. CMS-PAS-JME-16-003, 2017, http://cds.cern.ch/record/2256875.

[68] Y. L. Dokshitzer, G. D. Leder, S. Moretti, and B. R. Webber, Better jet clustering algorithms, J. High Energy Phys. 08 (1997) 001.

[69] M. Wobisch and T. Wengler, Hadronization corrections to jet cross sections in deep- inelastic scattering, arXiv:hep-ph/9907280.

[70] J. Thaler and K. Van Tilburg, Identifying boosted objects with N-subjettiness, J. High Energy Phys. 03 (2011) 015.

[71] T. Kam Ho, Random decision forests, *Proceedings of 3rd International Conference on Document Analysis and Recognition* (IEEE, New York, 1995), Vol. 1, p. 278.

[72] CMS Collaboration, CMS Physics Analysis Summary No. CMS-PAS-JME-13-002, 2013, https://cds.cern.ch/record/1599732.

[73] T. Junk, Confidence level computation for combining searches with small statistics, Nucl. Instrum. Methods Phys. Res., Sect. A **434**, 435 (1999).

[74] A. L. Read, Presentation of search results: The $CL_s$ technique, J. Phys. G **28**, 2693 (2002).

[75] ATLAS and CMS Collaborations, Technical Reports No. ATL-PHYS-PUB-2011-011, No. CMS NOTE-2011/005, 2011, https://cds.cern.ch/record/1379837.

[76] G. Cowan, K. Cranmer, E. Gross, and O. Vitells, Asymptotic formulae for likelihood-based tests of new physics, Eur. Phys. J. C **71**, 1554 (2011); Erratum, Eur. Phys. J. C **73**, 2501 (2013).

[77] CMS Collaboration (CMS), CMS Physics Analysis Summary No. CMS-PAS-LUM-17-001, 2017, https://cds.cern.ch/record/2257069.

[78] CMS Collaboration, Search for physics beyond the standard model in events with two leptons of same sign, missing transverse momentum, and jets in proton-proton collisions at $\sqrt{s} = 13$ TeV, Eur. Phys. J. C **77**, 578 (2017).

A. M. Sirunyan,[1] A. Tumasyan,[1] W. Adam,[2] F. Ambrogi,[2] E. Asilar,[2] T. Bergauer,[2] J. Brandstetter,[2] E. Brondolin,[2] M. Dragicevic,[2] J. Erö,[2] A. Escalante Del Valle,[2] M. Flechl,[2] M. Friedl,[2] R. Frühwirth,[2,b] V. M. Ghete,[2] J. Grossmann,[2] J. Hrubec,[2] M. Jeitler,[2,b] A. König,[2] N. Krammer,[2] I. Krätschmer,[2] D. Liko,[2] T. Madlener,[2] I. Mikulec,[2] E. Pree,[2] N. Rad,[2] H. Rohringer,[2] J. Schieck,[2,b] R. Schöfbeck,[2] M. Spanring,[2] D. Spitzbart,[2] W. Waltenberger,[2] J. Wittmann,[2] C.-E. Wulz,[2,b] M. Zarucki,[2] V. Chekhovsky,[3] V. Mossolov,[3] J. Suarez Gonzalez,[3] E. A. De Wolf,[4] D. Di Croce,[4] X. Janssen,[4] J. Lauwers,[4] M. Van De Klundert,[4] H. Van Haevermaet,[4] P. Van Mechelen,[4] N. Van Remortel,[4] S. Abu Zeid,[5] F. Blekman,[5] J. D'Hondt,[5] I. De Bruyn,[5] J. De Clercq,[5] K. Deroover,[5] G. Flouris,[5] D. Lontkovskyi,[5] S. Lowette,[5] I. Marchesini,[5] S. Moortgat,[5] L. Moreels,[5] Q. Python,[5] K. Skovpen,[5] S. Tavernier,[5] W. Van Doninck,[5] P. Van Mulders,[5] I. Van Parijs,[5] D. Beghin,[6] B. Bilin,[6] H. Brun,[6] B. Clerbaux,[6] G. De Lentdecker,[6] H. Delannoy,[6] B. Dorney,[6] G. Fasanella,[6] L. Favart,[6] R. Goldouzian,[6] A. Grebenyuk,[6] A. K. Kalsi,[6] T. Lenzi,[6] J. Luetic,[6] T. Maerschalk,[6] A. Marinov,[6] T. Seva,[6] E. Starling,[6] C. Vander Velde,[6] P. Vanlaer,[6] D. Vannerom,[6] R. Yonamine,[6] F. Zenoni,[6] T. Cornelis,[7] D. Dobur,[7] A. Fagot,[7] M. Gul,[7] I. Khvastunov,[7,c] D. Poyraz,[7] C. Roskas,[7] S. Salva,[7] M. Tytgat,[7] W. Verbeke,[7] N. Zaganidis,[7] H. Bakhshiansohi,[8] O. Bondu,[8] S. Brochet,[8] G. Bruno,[8] C. Caputo,[8] A. Caudron,[8] P. David,[8] S. De Visscher,[8] C. Delaere,[8] M. Delcourt,[8] B. Francois,[8] A. Giammanco,[8] M. Komm,[8] G. Krintiras,[8] V. Lemaitre,[8] A. Magitteri,[8] A. Mertens,[8] M. Musich,[8] K. Piotrzkowski,[8] L. Quertenmont,[8] A. Saggio,[8] M. Vidal Marono,[8] S. Wertz,[8] J. Zobec,[8] W. L. Aldá Júnior,[9] F. L. Alves,[9] G. A. Alves,[9] L. Brito,[9] M. Correa Martins Junior,[9] C. Hensel,[9] A. Moraes,[9] M. E. Pol,[9] P. Rebello Teles,[9] E. Belchior Batista Das Chagas,[10] W. Carvalho,[10] J. Chinellato,[10,d] E. Coelho,[10] E. M. Da Costa,[10] G. G. Da Silveira,[10,e] D. De Jesus Damiao,[10] S. Fonseca De Souza,[10] L. M. Huertas Guativa,[10] H. Malbouisson,[10] M. Melo De Almeida,[10] C. Mora Herrera,[10] L. Mundim,[10] H. Nogima,[10] L. J. Sanchez Rosas,[10] A. Santoro,[10] A. Sznajder,[10] M. Thiel,[10] E. J. Tonelli Manganote,[10,d] F. Torres Da Silva De Araujo,[10] A. Vilela Pereira,[10] S. Ahuja,[11a] C. A. Bernardes,[11a] T. R. Fernandez Perez Tomei,[11a] E. M. Gregores,[11b] P. G. Mercadante,[11b] S. F. Novaes,[11a] Sandra S. Padula,[11a] D. Romero Abad,[11b] J. C. Ruiz Vargas,[11a] A. Aleksandrov,[12] R. Hadjiiska,[12] P. Iaydjiev,[12] M. Misheva,[12] M. Rodozov,[12] M. Shopova,[12] G. Sultanov,[12] A. Dimitrov,[13] L. Litov,[13] B. Pavlov,[13] P. Petkov,[13] W. Fang,[14,f] X. Gao,[14,f] L. Yuan,[14] M. Ahmad,[15] J. G. Bian,[15] G. M. Chen,[15] H. S. Chen,[15] M. Chen,[15] Y. Chen,[15] C. H. Jiang,[15] D. Leggat,[15] H. Liao,[15] Z. Liu,[15] F. Romeo,[15] S. M. Shaheen,[15] A. Spiezia,[15] J. Tao,[15] C. Wang,[15] Z. Wang,[15] E. Yazgan,[15] H. Zhang,[15] S. Zhang,[15] J. Zhao,[15] Y. Ban,[16] G. Chen,[16] J. Li,[16] Q. Li,[16] S. Liu,[16] Y. Mao,[16] S. J. Qian,[16] D. Wang,[16] Z. Xu,[16] F. Zhang,[16,f] Y. Wang,[17] C. Avila,[18] A. Cabrera,[18] L. F. Chaparro Sierra,[18] C. Florez,[18] C. F. González Hernández,[18] J. D. Ruiz Alvarez,[18] M. A. Segura Delgado,[18] B. Courbon,[19] N. Godinovic,[19] D. Lelas,[19] I. Puljak,[19] P. M. Ribeiro Cipriano,[19] T. Sculac,[19] Z. Antunovic,[20] M. Kovac,[20] V. Brigljevic,[21] D. Ferencek,[21] K. Kadija,[21] B. Mesic,[21] A. Starodumov,[21,g] T. Susa,[21] M. W. Ather,[22] A. Attikis,[22] G. Mavromanolakis,[22] J. Mousa,[22] C. Nicolaou,[22] F. Ptochos,[22] P. A. Razis,[22] H. Rykaczewski,[22] M. Finger,[23,h] M. Finger Jr.,[23,h] E. Carrera Jarrin,[24] Y. Assran,[25,i,j] S. Elgammal,[25,j] A. Mahrous,[25,k] R. K. Dewanjee,[26] M. Kadastik,[26] L. Perrini,[26] M. Raidal,[26] A. Tiko,[26] C. Veelken,[26] P. Eerola,[27] H. Kirschenmann,[27] J. Pekkanen,[27] M. Voutilainen,[27] J. Havukainen,[28] J. K. Heikkilä,[28] T. Järvinen,[28] V. Karimäki,[28] R. Kinnunen,[28] T. Lampén,[28] K. Lassila-Perini,[28] S. Laurila,[28] S. Lehti,[28] T. Lindén,[28] P. Luukka,[28] H. Siikonen,[28] E. Tuominen,[28] J. Tuominiemi,[28] T. Tuuva,[29] M. Besancon,[30] F. Couderc,[30] M. Dejardin,[30] D. Denegri,[30] J. L. Faure,[30] F. Ferri,[30] S. Ganjour,[30] S. Ghosh,[30] P. Gras,[30] G. Hamel de Monchenault,[30] P. Jarry,[30] I. Kucher,[30] C. Leloup,[30] E. Locci,[30] M. Machet,[30] J. Malcles,[30] G. Negro,[30] J. Rander,[30] A. Rosowsky,[30] M. Ö. Sahin,[30] M. Titov,[30] A. Abdulsalam,[31] C. Amendola,[31] I. Antropov,[31] S. Baffioni,[31] F. Beaudette,[31] P. Busson,[31] L. Cadamuro,[31] C. Charlot,[31] R. Granier de Cassagnac,[31] M. Jo,[31] S. Lisniak,[31] A. Lobanov,[31] J. Martin Blanco,[31] M. Nguyen,[31] C. Ochando,[31] G. Ortona,[31] P. Paganini,[31] P. Pigard,[31] R. Salerno,[31] J. B. Sauvan,[31] Y. Sirois,[31] A. G. Stahl Leiton,[31] T. Strebler,[31] Y. Yilmaz,[31] A. Zabi,[31] A. Zghiche,[31] J.-L. Agram,[32,l] J. Andrea,[32] D. Bloch,[32] J.-M. Brom,[32] M. Buttignol,[32] E. C. Chabert,[32] N. Chanon,[32] C. Collard,[32] E. Conte,[32,l] X. Coubez,[32] J.-C. Fontaine,[32,l] D. Gelé,[32] U. Goerlach,[32] M. Jansová,[32] A.-C. Le Bihan,[32] N. Tonon,[32] P. Van Hove,[32] S. Gadrat,[33] S. Beauceron,[34] C. Bernet,[34] G. Boudoul,[34] R. Chierici,[34] D. Contardo,[34] P. Depasse,[34] H. El Mamouni,[34] J. Fay,[34] L. Finco,[34] S. Gascon,[34] M. Gouzevitch,[34] G. Grenier,[34] B. Ille,[34] F. Lagarde,[34] I. B. Laktineh,[34] M. Lethuillier,[34] L. Mirabito,[34] A. L. Pequegnot,[34] S. Perries,[34] A. Popov,[34,m] V. Sordini,[34] M. Vander Donckt,[34] S. Viret,[34] A. Khvedelidze,[35,h] Z. Tsamalaidze,[36,h] C. Autermann,[37] L. Feld,[37] M. K. Kiesel,[37] K. Klein,[37] M. Lipinski,[37] M. Preuten,[37] C. Schomakers,[37] J. Schulz,[37] M. Teroerde,[37] V. Zhukov,[37,m] A. Albert,[38] E. Dietz-Laursonn,[38] D. Duchardt,[38] M. Endres,[38] M. Erdmann,[38] S. Erdweg,[38] T. Esch,[38] R. Fischer,[38] A. Güth,[38] M. Hamer,[38] T. Hebbeker,[38] C. Heidemann,[38] K. Hoepfner,[38] S. Knutzen,[38] M. Merschmeyer,[38] A. Meyer,[38] P. Millet,[38] S. Mukherjee,[38] T. Pook,[38] M. Radziej,[38] H. Reithler,[38] M. Rieger,[38]

F. Scheuch,[38] D. Teyssier,[38] S. Thüer,[38] G. Flügge,[39] B. Kargoll,[39] T. Kress,[39] A. Künsken,[39] T. Müller,[39] A. Nehrkorn,[39] A. Nowack,[39] C. Pistone,[39] O. Pooth,[39] A. Stahl,[39,n] M. Aldaya Martin,[40] T. Arndt,[40] C. Asawatangtrakuldee,[40] K. Beernaert,[40] O. Behnke,[40] U. Behrens,[40] A. Bermúdez Martínez,[40] A. A. Bin Anuar,[40] K. Borras,[40,o] V. Botta,[40] A. Campbell,[40] P. Connor,[40] C. Contreras-Campana,[40] F. Costanza,[40] C. Diez Pardos,[40] G. Eckerlin,[40] D. Eckstein,[40] T. Eichhorn,[40] E. Eren,[40] E. Gallo,[40,p] J. Garay Garcia,[40] A. Geiser,[40] J. M. Grados Luyando,[40] A. Grohsjean,[40] P. Gunnellini,[40] M. Guthoff,[40] A. Harb,[40] J. Hauk,[40] M. Hempel,[40,q] H. Jung,[40] M. Kasemann,[40] J. Keaveney,[40] C. Kleinwort,[40] I. Korol,[40] D. Krücker,[40] W. Lange,[40] A. Lelek,[40] T. Lenz,[40] J. Leonard,[40] K. Lipka,[40] W. Lohmann,[40,q] R. Mankel,[40] I.-A. Melzer-Pellmann,[40] A. B. Meyer,[40] G. Mittag,[40] J. Mnich,[40] A. Mussgiller,[40] E. Ntomari,[40] D. Pitzl,[40] A. Raspereza,[40] M. Savitskyi,[40] P. Saxena,[40] R. Shevchenko,[40] N. Stefaniuk,[40] G. P. Van Onsem,[40] R. Walsh,[40] Y. Wen,[40] K. Wichmann,[40] C. Wissing,[40] O. Zenaiev,[40] R. Aggleton,[41] S. Bein,[41] V. Blobel,[41] M. Centis Vignali,[41] T. Dreyer,[41] E. Garutti,[41] D. Gonzalez,[41] J. Haller,[41] A. Hinzmann,[41] M. Hoffmann,[41] A. Karavdina,[41] R. Klanner,[41] R. Kogler,[41] N. Kovalchuk,[41] S. Kurz,[41] T. Lapsien,[41] D. Marconi,[41] M. Meyer,[41] M. Niedziela,[41] D. Nowatschin,[41] F. Pantaleo,[41,n] T. Peiffer,[41] A. Perieanu,[41] C. Scharf,[41] P. Schleper,[41] A. Schmidt,[41] S. Schumann,[41] J. Schwandt,[41] J. Sonneveld,[41] H. Stadie,[41] G. Steinbrück,[41] F. M. Stober,[41] M. Stöver,[41] H. Tholen,[41] D. Troendle,[41] E. Usai,[41] A. Vanhoefer,[41] B. Vormwald,[41] M. Akbiyik,[42] C. Barth,[42] M. Baselga,[42] S. Baur,[42] E. Butz,[42] R. Caspart,[42] T. Chwalek,[42] F. Colombo,[42] W. De Boer,[42] A. Dierlamm,[42] N. Faltermann,[42] B. Freund,[42] R. Friese,[42] M. Giffels,[42] M. A. Harrendorf,[42] F. Hartmann,[42,n] S. M. Heindl,[42] U. Husemann,[42] F. Kassel,[42,n] S. Kudella,[42] H. Mildner,[42] M. U. Mozer,[42] Th. Müller,[42] M. Plagge,[42] G. Quast,[42] K. Rabbertz,[42] M. Schröder,[42] I. Shvetsov,[42] G. Sieber,[42] H. J. Simonis,[42] R. Ulrich,[42] S. Wayand,[42] M. Weber,[42] T. Weiler,[42] S. Williamson,[42] C. Wöhrmann,[42] R. Wolf,[42] G. Anagnostou,[43] G. Daskalakis,[43] T. Geralis,[43] A. Kyriakis,[43] D. Loukas,[43] I. Topsis-Giotis,[43] G. Karathanasis,[44] S. Kesisoglou,[44] A. Panagiotou,[44] N. Saoulidou,[44] K. Kousouris,[45] I. Evangelou,[46] C. Foudas,[46] P. Gianneios,[46] P. Katsoulis,[46] P. Kokkas,[46] S. Mallios,[46] N. Manthos,[46] I. Papadopoulos,[46] E. Paradas,[46] J. Strologas,[46] F. A. Triantis,[46] D. Tsitsonis,[46] M. Csanad,[47] N. Filipovic,[47] G. Pasztor,[47] O. Surányi,[47] G. I. Veres,[47,r] G. Bencze,[48] C. Hajdu,[48] D. Horvath,[48,s] Á. Hunyadi,[48] F. Sikler,[48] V. Veszpremi,[48] N. Beni,[49] S. Czellar,[49] J. Karancsi,[49,t] A. Makovec,[49] J. Molnar,[49] Z. Szillasi,[49] M. Bartók,[50,r] P. Raics,[50] Z. L. Trocsanyi,[50] B. Ujvari,[50] S. Choudhury,[51] J. R. Komaragiri,[51] S. Bahinipati,[52,u] S. Bhowmik,[52] P. Mal,[52] K. Mandal,[52] A. Nayak,[52,v] D. K. Sahoo,[52,u] N. Sahoo,[52] S. K. Swain,[52] S. Bansal,[53] S. B. Beri,[53] V. Bhatnagar,[53] R. Chawla,[53] N. Dhingra,[53] A. Kaur,[53] M. Kaur,[53] S. Kaur,[53] R. Kumar,[53] P. Kumari,[53] A. Mehta,[53] J. B. Singh,[53] G. Walia,[53] Ashok Kumar,[54] Aashaq Shah,[54] A. Bhardwaj,[54] S. Chauhan,[54] B. C. Choudhary,[54] R. B. Garg,[54] S. Keshri,[54] A. Kumar,[54] S. Malhotra,[54] M. Naimuddin,[54] K. Ranjan,[54] R. Sharma,[54] R. Bhardwaj,[55] R. Bhattacharya,[55] S. Bhattacharya,[55] U. Bhawandeep,[55] S. Dey,[55] S. Dutt,[55] S. Dutta,[55] S. Ghosh,[55] N. Majumdar,[55] A. Modak,[55] K. Mondal,[55] S. Mukhopadhyay,[55] S. Nandan,[55] A. Purohit,[55] A. Roy,[55] S. Roy Chowdhury,[55] S. Sarkar,[55] M. Sharan,[55] S. Thakur,[55] P. K. Behera,[56] R. Chudasama,[57] D. Dutta,[57] V. Jha,[57] V. Kumar,[57] A. K. Mohanty,[57,n] P. K. Netrakanti,[57] L. M. Pant,[57] P. Shukla,[57] A. Topkar,[57] T. Aziz,[58] S. Dugad,[58] B. Mahakud,[58] S. Mitra,[58] G. B. Mohanty,[58] N. Sur,[58] B. Sutar,[58] S. Banerjee,[59] S. Bhattacharya,[59] S. Chatterjee,[59] P. Das,[59] M. Guchait,[59] Sa. Jain,[59] S. Kumar,[59] M. Maity,[59,w] G. Majumder,[59] K. Mazumdar,[59] T. Sarkar,[59,w] N. Wickramage,[59,x] S. Chauhan,[60] S. Dube,[60] V. Hegde,[60] A. Kapoor,[60] K. Kothekar,[60] S. Pandey,[60] A. Rane,[60] S. Sharma,[60] S. Chenarani,[61,y] E. Eskandari Tadavani,[61] S. M. Etesami,[61,y] M. Khakzad,[61] M. Mohammadi Najafabadi,[61] M. Naseri,[61] S. Paktinat Mehdiabadi,[61,z] F. Rezaei Hosseinabadi,[61] B. Safarzadeh,[61,aa] M. Zeinali,[61] M. Felcini,[62] M. Grunewald,[62] M. Abbrescia,[63a,63b] C. Calabria,[63a,63b] A. Colaleo,[63a] D. Creanza,[63a,63c] L. Cristella,[63a,63b] N. De Filippis,[63a,63c] M. De Palma,[63a,63b] F. Errico,[63a,63b] L. Fiore,[63a] G. Iaselli,[63a,63c] S. Lezki,[63a,63b] G. Maggi,[63a,63c] M. Maggi,[63a] G. Miniello,[63a,63b] S. My,[63a,63b] S. Nuzzo,[63a,63b] A. Pompili,[63a,63b] G. Pugliese,[63a,63c] R. Radogna,[63a] A. Ranieri,[63a] G. Selvaggi,[63a,63b] A. Sharma,[63a] L. Silvestris,[63a,n] R. Venditti,[63a] P. Verwilligen,[63a] G. Abbiendi,[64a] C. Battilana,[64a,64b] D. Bonacorsi,[64a,64b] L. Borgonovi,[64a,64b] S. Braibant-Giacomelli,[64a,64b] R. Campanini,[64a,64b] P. Capiluppi,[64a,64b] A. Castro,[64a,64b] F. R. Cavallo,[64a] S. S. Chhibra,[64a] G. Codispoti,[64a,64b] M. Cuffiani,[64a,64b] G. M. Dallavalle,[64a] F. Fabbri,[64a] A. Fanfani,[64a,64b] D. Fasanella,[64a,64b] P. Giacomelli,[64a] C. Grandi,[64a] L. Guiducci,[64a,64b] S. Marcellini,[64a] G. Masetti,[64a] A. Montanari,[64a] F. L. Navarria,[64a,64b] A. Perrotta,[64a] A. M. Rossi,[64a,64b] T. Rovelli,[64a,64b] G. P. Siroli,[64a,64b] N. Tosi,[64a] S. Albergo,[65a,65b] S. Costa,[65a,65b] A. Di Mattia,[65a] F. Giordano,[65a,65b] R. Potenza,[65a,65b] A. Tricomi,[65a,65b] C. Tuve,[65a,65b] G. Barbagli,[66a] K. Chatterjee,[66a,66b] V. Ciulli,[66a,66b] C. Civinini,[66a] R. D'Alessandro,[66a,66b] E. Focardi,[66a,66b] P. Lenzi,[66a,66b] M. Meschini,[66a] S. Paoletti,[66a] L. Russo,[66a,bb] G. Sguazzoni,[66a] D. Strom,[66a] L. Viliani,[66a] L. Benussi,[67] S. Bianco,[67] F. Fabbri,[67] D. Piccolo,[67] F. Primavera,[67,n] V. Calvelli,[68a,68b] F. Ferro,[68a] F. Ravera,[68a,68b] E. Robutti,[68a] S. Tosi,[68a,68b]

A. Benaglia,[69a] A. Beschi,[69b] L. Brianza,[69a,69b] F. Brivio,[69a,69b] V. Ciriolo,[69a,69b,n] M. E. Dinardo,[69a,69b] S. Fiorendi,[69a,69b] S. Gennai,[69a] A. Ghezzi,[69a,69b] P. Govoni,[69a,69b] M. Malberti,[69a,69b] S. Malvezzi,[69a] R. A. Manzoni,[69a,69b] D. Menasce,[69a] L. Moroni,[69a] M. Paganoni,[69a,69b] K. Pauwels,[69a,69b] D. Pedrini,[69a] S. Pigazzini,[69a,69b,cc] S. Ragazzi,[69a,69b] T. Tabarelli de Fatis,[69a,69b] S. Buontempo,[70a] N. Cavallo,[70a,70c] S. Di Guida,[70a,70d,n] F. Fabozzi,[70a,70c] F. Fienga,[70a,70b] A. O. M. Iorio,[70a,70b] W. A. Khan,[70a] L. Lista,[70a] S. Meola,[70a,70d,n] P. Paolucci,[70a,n] C. Sciacca,[70a,70b] F. Thyssen,[70a] P. Azzi,[71a] N. Bacchetta,[71a] L. Benato,[71a,71b] D. Bisello,[71a,71b] A. Boletti,[71a,71b] R. Carlin,[71a,71b] A. Carvalho Antunes De Oliveira,[71a,71b] P. Checchia,[71a] P. De Castro Manzano,[71a] T. Dorigo,[71a] U. Dosselli,[71a] F. Gasparini,[71a,71b] U. Gasparini,[71a,71b] A. Gozzelino,[71a] S. Lacaprara,[71a] M. Margoni,[71a,71b] A. T. Meneguzzo,[71a,71b] N. Pozzobon,[71a,71b] P. Ronchese,[71a,71b] R. Rossin,[71a,71b] F. Simonetto,[71a,71b] E. Torassa,[71a] M. Zanetti,[71a,71b] P. Zotto,[71a,71b] G. Zumerle,[71a,71b] A. Braghieri,[72a] A. Magnani,[72a] P. Montagna,[72a,72b] S. P. Ratti,[72a,72b] V. Re,[72a] M. Ressegotti,[72a,72b] C. Riccardi,[72a,72b] P. Salvini,[72a] I. Vai,[72a,72b] P. Vitulo,[72a,72b] L. Alunni Solestizi,[73a,73b] M. Biasini,[73a,73b] G. M. Bilei,[73a] C. Cecchi,[73a,73b] D. Ciangottini,[73a,73b] L. Fanò,[73a,73b] R. Leonardi,[73a,73b] E. Manoni,[73a] G. Mantovani,[73a,73b] V. Mariani,[73a,73b] M. Menichelli,[73a] A. Rossi,[73a,73b] A. Santocchia,[73a,73b] D. Spiga,[73a] K. Androsov,[74a] P. Azzurri,[74a,n] G. Bagliesi,[74a] T. Boccali,[74a] L. Borrello,[74a] R. Castaldi,[74a] M. A. Ciocci,[74a,74b] R. Dell'Orso,[74a] G. Fedi,[74a] L. Giannini,[74a,74c] A. Giassi,[74a] M. T. Grippo,[74a,bb] F. Ligabue,[74a,74c] T. Lomtadze,[74a] E. Manca,[74a,74c] G. Mandorli,[74a,74c] A. Messineo,[74a,74b] F. Palla,[74a] A. Rizzi,[74a,74b] A. Savoy-Navarro,[74a,dd] P. Spagnolo,[74a] R. Tenchini,[74a] G. Tonelli,[74a,74b] A. Venturi,[74a] P. G. Verdini,[74a] L. Barone,[75a,75b] F. Cavallari,[75a] M. Cipriani,[75a,75b] N. Daci,[75a] D. Del Re,[75a,75b,n] E. Di Marco,[75a,75b] M. Diemoz,[75a] S. Gelli,[75a,75b] E. Longo,[75a,75b] F. Margaroli,[75a,75b] B. Marzocchi,[75a,75b] P. Meridiani,[75a] G. Organtini,[75a,75b] R. Paramatti,[75a,75b] F. Preiato,[75a,75b] S. Rahatlou,[75a,75b] C. Rovelli,[75a] F. Santanastasio,[75a,75b] N. Amapane,[76a,76b] R. Arcidiacono,[76a,76c] S. Argiro,[76a,76b] M. Arneodo,[76a,76c] N. Bartosik,[76a] R. Bellan,[76a,76b] C. Biino,[76a] N. Cartiglia,[76a] F. Cenna,[76a,76b] M. Costa,[76a,76b] R. Covarelli,[76a,76b] A. Degano,[76a,76b] N. Demaria,[76a] B. Kiani,[76a,76b] C. Mariotti,[76a] S. Maselli,[76a] E. Migliore,[76a,76b] V. Monaco,[76a,76b] E. Monteil,[76a,76b] M. Monteno,[76a] M. M. Obertino,[76a,76b] L. Pacher,[76a,76b] N. Pastrone,[76a] M. Pelliccioni,[76a] G. L. Pinna Angioni,[76a,76b] A. Romero,[76a,76b] M. Ruspa,[76a,76c] R. Sacchi,[76a,76b] K. Shchelina,[76a,76b] V. Sola,[76a] A. Solano,[76a,76b] A. Staiano,[76a] P. Traczyk,[76a,76b] S. Belforte,[77a] M. Casarsa,[77a] F. Cossutti,[77a] G. Della Ricca,[77a,77b] A. Zanetti,[77a] D. H. Kim,[78] G. N. Kim,[78] M. S. Kim,[78] J. Lee,[78] S. Lee,[78] S. W. Lee,[78] C. S. Moon,[78] Y. D. Oh,[78] S. Sekmen,[78] D. C. Son,[78] Y. C. Yang,[78] A. Lee,[79] H. Kim,[80] D. H. Moon,[80] G. Oh,[80] J. A. Brochero Cifuentes,[81] J. Goh,[81] T. J. Kim,[81] S. Cho,[82] S. Choi,[82] Y. Go,[82] D. Gyun,[82] S. Ha,[82] B. Hong,[82] Y. Jo,[82] Y. Kim,[82] K. Lee,[82] K. S. Lee,[82] S. Lee,[82] J. Lim,[82] S. K. Park,[82] Y. Roh,[82] J. Almond,[83] J. Kim,[83] J. S. Kim,[83] H. Lee,[83] K. Lee,[83] K. Nam,[83] S. B. Oh,[83] B. C. Radburn-Smith,[83] S. h. Seo,[83] U.K. Yang,[83] H. D. Yoo,[83] G. B. Yu,[83] H. Kim,[84] J. H. Kim,[84] J. S. H. Lee,[84] I. C. Park,[84] Y. Choi,[85] C. Hwang,[85] J. Lee,[85] I. Yu,[85] V. Dudenas,[86] A. Juodagalvis,[86] J. Vaitkus,[86] I. Ahmed,[87] Z. A. Ibrahim,[87] M. A. B. Md Ali,[87,ee] F. Mohamad Idris,[87,ff] W. A. T. Wan Abdullah,[87] M. N. Yusli,[87] Z. Zolkapli,[87] R Reyes-Almanza,[88] G. Ramirez-Sanchez,[88] M. C. Duran-Osuna,[88] H. Castilla-Valdez,[88] E. De La Cruz-Burelo,[88] I. Heredia-De La Cruz,[88,gg] R. I. Rabadan-Trejo,[88] R. Lopez-Fernandez,[88] J. Mejia Guisao,[88] A. Sanchez-Hernandez,[88] S. Carrillo Moreno,[89] C. Oropeza Barrera,[89] F. Vazquez Valencia,[89] J. Eysermans,[90] I. Pedraza,[90] H. A. Salazar Ibarguen,[90] C. Uribe Estrada,[90] A. Morelos Pineda,[91] D. Krofcheck,[92] P. H. Butler,[93] A. Ahmad,[94] M. Ahmad,[94] Q. Hassan,[94] H. R. Hoorani,[94] A. Saddique,[94] M. A. Shah,[94] M. Shoaib,[94] M. Waqas,[94] H. Bialkowska,[95] M. Bluj,[95] B. Boimska,[95] T. Frueboes,[95] M. Górski,[95] M. Kazana,[95] K. Nawrocki,[95] M. Szleper,[95] P. Zalewski,[95] K. Bunkowski,[96] A. Byszuk,[96,hh] K. Doroba,[96] A. Kalinowski,[96] M. Konecki,[96] J. Krolikowski,[96] M. Misiura,[96] M. Olszewski,[96] A. Pyskir,[96] M. Walczak,[96] P. Bargassa,[97] C. Beirão Da Cruz E Silva,[97] A. Di Francesco,[97] P. Faccioli,[97] B. Galinhas,[97] M. Gallinaro,[97] J. Hollar,[97] N. Leonardo,[97] L. Lloret Iglesias,[97] M. V. Nemallapudi,[97] J. Seixas,[97] G. Strong,[97] O. Toldaiev,[97] D. Vadruccio,[97] J. Varela,[97] S. Afanasiev,[98] V. Alexakhin,[98] A. Golunov,[98] I. Golutvin,[98] N. Gorbounov,[98] A. Kamenev,[98] V. Karjavin,[98] A. Lanev,[98] A. Malakhov,[98] V. Matveev,[98,ii,jj] V. Palichik,[98] V. Perelygin,[98] M. Savina,[98] S. Shmatov,[98] S. Shulha,[98] N. Skatchkov,[98] V. Smirnov,[98] A. Zarubin,[98] Y. Ivanov,[99] V. Kim,[99,kk] E. Kuznetsova,[99,ll] P. Levchenko,[99] V. Murzin,[99] V. Oreshkin,[99] I. Smirnov,[99] D. Sosnov,[99] V. Sulimov,[99] L. Uvarov,[99] S. Vavilov,[99] A. Vorobyev,[99] Yu. Andreev,[100] A. Dermenev,[100] S. Gninenko,[100] N. Golubev,[100] A. Karneyeu,[100] M. Kirsanov,[100] N. Krasnikov,[100] A. Pashenkov,[100] D. Tlisov,[100] A. Toropin,[100] V. Epshteyn,[101] V. Gavrilov,[101] N. Lychkovskaya,[101] V. Popov,[101] I. Pozdnyakov,[101] G. Safronov,[101] A. Spiridonov,[101] A. Stepennov,[101] M. Toms,[101] E. Vlasov,[101] A. Zhokin,[101] T. Aushev,[102] A. Bylinkin,[102,jj] R. Chistov,[103,mm] M. Danilov,[103,mm] P. Parygin,[103] D. Philippov,[103] S. Polikarpov,[103] E. Tarkovskii,[103] V. Andreev,[104] M. Azarkin,[104,jj] I. Dremin,[104,jj] M. Kirakosyan,[104,jj] A. Terkulov,[104] A. Baskakov,[105] A. Belyaev,[105] E. Boos,[105] V. Bunichev,[105] M. Dubinin,[105,nn] L. Dudko,[105] A. Gribushin,[105]

V. Klyukhin,[105] O. Kodolova,[105] I. Lokhtin,[105] I. Miagkov,[105] S. Obraztsov,[105] M. Perfilov,[105] V. Savrin,[105] A. Snigirev,[105] V. Blinov,[106,oo] Y. Skovpen,[106,oo] D. Shtol,[106,oo] I. Azhgirey,[107] I. Bayshev,[107] S. Bitioukov,[107] D. Elumakhov,[107] A. Godizov,[107] V. Kachanov,[107] A. Kalinin,[107] D. Konstantinov,[107] P. Mandrik,[107] V. Petrov,[107] R. Ryutin,[107] A. Sobol,[107] S. Troshin,[107] N. Tyurin,[107] A. Uzunian,[107] A. Volkov,[107] P. Adzic,[108,pp] P. Cirkovic,[108] D. Devetak,[108] M. Dordevic,[108] J. Milosevic,[108] V. Rekovic,[108] J. Alcaraz Maestre,[109] I. Bachiller,[109] M. Barrio Luna,[109] M. Cerrada,[109] N. Colino,[109] B. De La Cruz,[109] A. Delgado Peris,[109] C. Fernandez Bedoya,[109] J. P. Fernández Ramos,[109] J. Flix,[109] M. C. Fouz,[109] O. Gonzalez Lopez,[109] S. Goy Lopez,[109] J. M. Hernandez,[109] M. I. Josa,[109] D. Moran,[109] A. Pérez-Calero Yzquierdo,[109] J. Puerta Pelayo,[109] A. Quintario Olmeda,[109] I. Redondo,[109] L. Romero,[109] M. S. Soares,[109] A. Álvarez Fernández,[109] C. Albajar,[110] J. F. de Trocóniz,[110] M. Missiroli,[110] J. Cuevas,[111] C. Erice,[111] J. Fernandez Menendez,[111] I. Gonzalez Caballero,[111] J. R. González Fernández,[111] E. Palencia Cortezon,[111] S. Sanchez Cruz,[111] P. Vischia,[111] J. M. Vizan Garcia,[111] I. J. Cabrillo,[112] A. Calderon,[112] B. Chazin Quero,[112] E. Curras,[112] J. Duarte Campderros,[112] M. Fernandez,[112] J. Garcia-Ferrero,[112] G. Gomez,[112] A. Lopez Virto,[112] J. Marco,[112] C. Martinez Rivero,[112] P. Martinez Ruiz del Arbol,[112] F. Matorras,[112] J. Piedra Gomez,[112] T. Rodrigo,[112] A. Ruiz-Jimeno,[112] L. Scodellaro,[112] N. Trevisani,[112] I. Vila,[112] R. Vilar Cortabitarte,[112] D. Abbaneo,[113] B. Akgun,[113] E. Auffray,[113] P. Baillon,[113] A. H. Ball,[113] D. Barney,[113] J. Bendavid,[113] M. Bianco,[113] P. Bloch,[113] A. Bocci,[113] C. Botta,[113] T. Camporesi,[113] R. Castello,[113] M. Cepeda,[113] G. Cerminara,[113] E. Chapon,[113] Y. Chen,[113] D. d'Enterria,[113] A. Dabrowski,[113] V. Daponte,[113] A. David,[113] M. De Gruttola,[113] A. De Roeck,[113] N. Deelen,[113] M. Dobson,[113] T. du Pree,[113] M. Dünser,[113] N. Dupont,[113] A. Elliott-Peisert,[113] P. Everaerts,[113] F. Fallavollita,[113] G. Franzoni,[113] J. Fulcher,[113] W. Funk,[113] D. Gigi,[113] A. Gilbert,[113] K. Gill,[113] F. Glege,[113] D. Gulhan,[113] P. Harris,[113] J. Hegeman,[113] V. Innocente,[113] A. Jafari,[113] P. Janot,[113] O. Karacheban,[113,q] J. Kieseler,[113] V. Knünz,[113] A. Kornmayer,[113] M. J. Kortelainen,[113] M. Krammer,[113,b] C. Lange,[113] P. Lecoq,[113] C. Lourenço,[113] M. T. Lucchini,[113] L. Malgeri,[113] M. Mannelli,[113] A. Martelli,[113] F. Meijers,[113] J. A. Merlin,[113] S. Mersi,[113] E. Meschi,[113] P. Milenovic,[113,qq] F. Moortgat,[113] M. Mulders,[113] H. Neugebauer,[113] J. Ngadiuba,[113] S. Orfanelli,[113] L. Orsini,[113] L. Pape,[113] E. Perez,[113] M. Peruzzi,[113] A. Petrilli,[113] G. Petrucciani,[113] A. Pfeiffer,[113] M. Pierini,[113] D. Rabady,[113] A. Racz,[113] T. Reis,[113] G. Rolandi,[113,rr] M. Rovere,[113] H. Sakulin,[113] C. Schäfer,[113] C. Schwick,[113] M. Seidel,[113] M. Selvaggi,[113] A. Sharma,[113] P. Silva,[113] P. Sphicas,[113,ss] A. Stakia,[113] J. Steggemann,[113] M. Stoye,[113] M. Tosi,[113] D. Treille,[113] A. Triossi,[113] A. Tsirou,[113] V. Veckalns,[113,tt] M. Verweij,[113] W. D. Zeuner,[113] W. Bertl,[114,a] L. Caminada,[114,uu] K. Deiters,[114] W. Erdmann,[114] R. Horisberger,[114] Q. Ingram,[114] H. C. Kaestli,[114] D. Kotlinski,[114] U. Langenegger,[114] T. Rohe,[114] S. A. Wiederkehr,[114] M. Backhaus,[115] L. Bäni,[115] P. Berger,[115] L. Bianchini,[115] B. Casal,[115] G. Dissertori,[115] M. Dittmar,[115] M. Donegà,[115] C. Dorfer,[115] C. Grab,[115] C. Heidegger,[115] D. Hits,[115] J. Hoss,[115] G. Kasieczka,[115] T. Klijnsma,[115] W. Lustermann,[115] B. Mangano,[115] M. Marionneau,[115] M. T. Meinhard,[115] D. Meister,[115] F. Micheli,[115] P. Musella,[115] F. Nessi-Tedaldi,[115] F. Pandolfi,[115] J. Pata,[115] F. Pauss,[115] G. Perrin,[115] L. Perrozzi,[115] M. Quittnat,[115] M. Reichmann,[115] D. A. Sanz Becerra,[115] M. Schönenberger,[115] L. Shchutska,[115] V. R. Tavolaro,[115] K. Theofilatos,[115] M. L. Vesterbacka Olsson,[115] R. Wallny,[115] D. H. Zhu,[115] T. K. Aarrestad,[116] C. Amsler,[116,vv] M. F. Canelli,[116] A. De Cosa,[116] R. Del Burgo,[116] S. Donato,[116] C. Galloni,[116] T. Hreus,[116] B. Kilminster,[116] D. Pinna,[116] G. Rauco,[116] P. Robmann,[116] D. Salerno,[116] K. Schweiger,[116] C. Seitz,[116] Y. Takahashi,[116] A. Zucchetta,[116] V. Candelise,[117] Y. H. Chang,[117] K. y. Cheng,[117] T. H. Doan,[117] Sh. Jain,[117] R. Khurana,[117] C. M. Kuo,[117] W. Lin,[117] A. Pozdnyakov,[117] S. S. Yu,[117] Arun Kumar,[118] P. Chang,[118] Y. Chao,[118] K. F. Chen,[118] P. H. Chen,[118] F. Fiori,[118] W.-S. Hou,[118] Y. Hsiung,[118] Y. F. Liu,[118] R.-S. Lu,[118] E. Paganis,[118] A. Psallidas,[118] A. Steen,[118] J. f. Tsai,[118] B. Asavapibhop,[119] K. Kovitanggoon,[119] G. Singh,[119] N. Srimanobhas,[119] M. N. Bakirci,[120,ww] A. Bat,[120] F. Boran,[120] S. Damarseckin,[120] Z. S. Demiroglu,[120] C. Dozen,[120] S. Girgis,[120] G. Gokbulut,[120] Y. Guler,[120] I. Hos,[120,xx] E. E. Kangal,[120,yy] O. Kara,[120] U. Kiminsu,[120] M. Oglakci,[120] G. Onengut,[120,zz] K. Ozdemir,[120,aaa] S. Ozturk,[120,ww] A. Polatoz,[120] B. Tali,[120,bbb] U. G. Tok,[120] H. Topakli,[120,ww] S. Turkcapar,[120] I. S. Zorbakir,[120] C. Zorbilmez,[120] G. Karapinar,[121,ccc] K. Ocalan,[121,ddd] M. Yalvac,[121] M. Zeyrek,[121] E. Gülmez,[122] M. Kaya,[122,eee] O. Kaya,[122,fff] S. Tekten,[122] E. A. Yetkin,[122,ggg] M. N. Agaras,[123] S. Atay,[123] A. Cakir,[123] K. Cankocak,[123] I. Köseoglu,[123] B. Grynyov,[124] L. Levchuk,[125] F. Ball,[126] L. Beck,[126] J. J. Brooke,[126] D. Burns,[126] E. Clement,[126] D. Cussans,[126] O. Davignon,[126] H. Flacher,[126] J. Goldstein,[126] G. P. Heath,[126] H. F. Heath,[126] L. Kreczko,[126] D. M. Newbold,[126,hhh] S. Paramesvaran,[126] T. Sakuma,[126] S. Seif El Nasr-storey,[126] D. Smith,[126] V. J. Smith,[126] K. W. Bell,[127] A. Belyaev,[127,iii] C. Brew,[127] R. M. Brown,[127] L. Calligaris,[127] D. Cieri,[127] D. J. A. Cockerill,[127] J. A. Coughlan,[127] K. Harder,[127] S. Harper,[127] J. Linacre,[127] E. Olaiya,[127] D. Petyt,[127] C. H. Shepherd-Themistocleous,[127] A. Thea,[127] I. R. Tomalin,[127] T. Williams,[127] G. Auzinger,[128]

R. Bainbridge,[128] J. Borg,[128] S. Breeze,[128] O. Buchmuller,[128] A. Bundock,[128] S. Casasso,[128] M. Citron,[128] D. Colling,[128] L. Corpe,[128] P. Dauncey,[128] G. Davies,[128] A. De Wit,[128] M. Della Negra,[128] R. Di Maria,[128] A. Elwood,[128] Y. Haddad,[128] G. Hall,[128] G. Iles,[128] T. James,[128] R. Lane,[128] C. Laner,[128] L. Lyons,[128] A.-M. Magnan,[128] S. Malik,[128] L. Mastrolorenzo,[128] T. Matsushita,[128] J. Nash,[128] A. Nikitenko,[128,g] V. Palladino,[128] M. Pesaresi,[128] D. M. Raymond,[128] A. Richards,[128] A. Rose,[128] E. Scott,[128] C. Seez,[128] A. Shtipliyski,[128] S. Summers,[128] A. Tapper,[128] K. Uchida,[128] M. Vazquez Acosta,[128,jjj] T. Virdee,[128,n] N. Wardle,[128] D. Winterbottom,[128] J. Wright,[128] S. C. Zenz,[128] J. E. Cole,[129] P. R. Hobson,[129] A. Khan,[129] P. Kyberd,[129] I. D. Reid,[129] L. Teodorescu,[129] S. Zahid,[129] A. Borzou,[130] K. Call,[130] J. Dittmann,[130] K. Hatakeyama,[130] H. Liu,[130] N. Pastika,[130] C. Smith,[130] R. Bartek,[131] A. Dominguez,[131] A. Buccilli,[132] S. I. Cooper,[132] C. Henderson,[132] P. Rumerio,[132] C. West,[132] D. Arcaro,[133] A. Avetisyan,[133] T. Bose,[133] D. Gastler,[133] D. Rankin,[133] C. Richardson,[133] J. Rohlf,[133] L. Sulak,[133] D. Zou,[133] G. Benelli,[134] D. Cutts,[134] A. Garabedian,[134] M. Hadley,[134] J. Hakala,[134] U. Heintz,[134] J. M. Hogan,[134] K. H. M. Kwok,[134] E. Laird,[134] G. Landsberg,[134] J. Lee,[134] Z. Mao,[134] M. Narain,[134] J. Pazzini,[134] S. Piperov,[134] S. Sagir,[134] R. Syarif,[134] D. Yu,[134] R. Band,[135] C. Brainerd,[135] R. Breedon,[135] D. Burns,[135] M. Calderon De La Barca Sanchez,[135] M. Chertok,[135] J. Conway,[135] R. Conway,[135] P. T. Cox,[135] R. Erbacher,[135] C. Flores,[135] G. Funk,[135] W. Ko,[135] R. Lander,[135] C. Mclean,[135] M. Mulhearn,[135] D. Pellett,[135] J. Pilot,[135] S. Shalhout,[135] M. Shi,[135] J. Smith,[135] D. Stolp,[135] K. Tos,[135] M. Tripathi,[135] Z. Wang,[135] M. Bachtis,[136] C. Bravo,[136] R. Cousins,[136] A. Dasgupta,[136] A. Florent,[136] J. Hauser,[136] M. Ignatenko,[136] N. Mccoll,[136] S. Regnard,[136] D. Saltzberg,[136] C. Schnaible,[136] V. Valuev,[136] E. Bouvier,[137] K. Burt,[137] R. Clare,[137] J. Ellison,[137] J. W. Gary,[137] S. M. A. Ghiasi Shirazi,[137] G. Hanson,[137] J. Heilman,[137] G. Karapostoli,[137] E. Kennedy,[137] F. Lacroix,[137] O. R. Long,[137] M. Olmedo Negrete,[137] M. I. Paneva,[137] W. Si,[137] L. Wang,[137] H. Wei,[137] S. Wimpenny,[137] B. R. Yates,[137] J. G. Branson,[138] S. Cittolin,[138] M. Derdzinski,[138] R. Gerosa,[138] D. Gilbert,[138] B. Hashemi,[138] A. Holzner,[138] D. Klein,[138] G. Kole,[138] V. Krutelyov,[138] J. Letts,[138] M. Masciovecchio,[138] D. Olivito,[138] S. Padhi,[138] M. Pieri,[138] M. Sani,[138] V. Sharma,[138] M. Tadel,[138] A. Vartak,[138] S. Wasserbaech,[138,kkk] J. Wood,[138] F. Würthwein,[138] A. Yagil,[138] G. Zevi Della Porta,[138] N. Amin,[139] R. Bhandari,[139] J. Bradmiller-Feld,[139] C. Campagnari,[139] A. Dishaw,[139] V. Dutta,[139] M. Franco Sevilla,[139] L. Gouskos,[139] R. Heller,[139] J. Incandela,[139] A. Ovcharova,[139] H. Qu,[139] J. Richman,[139] D. Stuart,[139] I. Suarez,[139] J. Yoo,[139] D. Anderson,[140] A. Bornheim,[140] J. M. Lawhorn,[140] H. B. Newman,[140] T. Q. Nguyen,[140] C. Pena,[140] M. Spiropulu,[140] J. R. Vlimant,[140] S. Xie,[140] Z. Zhang,[140] R. Y. Zhu,[140] M. B. Andrews,[141] T. Ferguson,[141] T. Mudholkar,[141] M. Paulini,[141] J. Russ,[141] M. Sun,[141] H. Vogel,[141] I. Vorobiev,[141] M. Weinberg,[141] J. P. Cumalat,[142] W. T. Ford,[142] F. Jensen,[142] A. Johnson,[142] M. Krohn,[142] S. Leontsinis,[142] T. Mulholland,[142] K. Stenson,[142] S. R. Wagner,[142] J. Alexander,[143] J. Chaves,[143] J. Chu,[143] S. Dittmer,[143] K. Mcdermott,[143] N. Mirman,[143] J. R. Patterson,[143] D. Quach,[143] A. Rinkevicius,[143] A. Ryd,[143] L. Skinnari,[143] L. Soffi,[143] S. M. Tan,[143] Z. Tao,[143] J. Thom,[143] J. Tucker,[143] P. Wittich,[143] M. Zientek,[143] S. Abdullin,[144] M. Albrow,[144] M. Alyari,[144] G. Apollinari,[144] A. Apresyan,[144] A. Apyan,[144] S. Banerjee,[144] L. A. T. Bauerdick,[144] A. Beretvas,[144] J. Berryhill,[144] P. C. Bhat,[144] G. Bolla,[144,a] K. Burkett,[144] J. N. Butler,[144] A. Canepa,[144] G. B. Cerati,[144] H. W. K. Cheung,[144] F. Chlebana,[144] M. Cremonesi,[144] J. Duarte,[144] V. D. Elvira,[144] J. Freeman,[144] Z. Gecse,[144] E. Gottschalk,[144] L. Gray,[144] D. Green,[144] S. Grünendahl,[144] O. Gutsche,[144] R. M. Harris,[144] S. Hasegawa,[144] J. Hirschauer,[144] Z. Hu,[144] B. Jayatilaka,[144] S. Jindariani,[144] M. Johnson,[144] U. Joshi,[144] B. Klima,[144] B. Kreis,[144] S. Lammel,[144] D. Lincoln,[144] R. Lipton,[144] M. Liu,[144] T. Liu,[144] R. Lopes De Sá,[144] J. Lykken,[144] K. Maeshima,[144] N. Magini,[144] J. M. Marraffino,[144] D. Mason,[144] P. McBride,[144] P. Merkel,[144] S. Mrenna,[144] S. Nahn,[144] V. O'Dell,[144] K. Pedro,[144] O. Prokofyev,[144] G. Rakness,[144] L. Ristori,[144] B. Schneider,[144] E. Sexton-Kennedy,[144] A. Soha,[144] W. J. Spalding,[144] L. Spiegel,[144] S. Stoynev,[144] J. Strait,[144] N. Strobbe,[144] L. Taylor,[144] S. Tkaczyk,[144] N. V. Tran,[144] L. Uplegger,[144] E. W. Vaandering,[144] C. Vernieri,[144] M. Verzocchi,[144] R. Vidal,[144] M. Wang,[144] H. A. Weber,[144] A. Whitbeck,[144] D. Acosta,[145] P. Avery,[145] P. Bortignon,[145] D. Bourilkov,[145] A. Brinkerhoff,[145] A. Carnes,[145] M. Carver,[145] D. Curry,[145] R. D. Field,[145] I. K. Furic,[145] S. V. Gleyzer,[145] B. M. Joshi,[145] J. Konigsberg,[145] A. Korytov,[145] K. Kotov,[145] P. Ma,[145] K. Matchev,[145] H. Mei,[145] G. Mitselmakher,[145] K. Shi,[145] D. Sperka,[145] N. Terentyev,[145] L. Thomas,[145] J. Wang,[145] S. Wang,[145] J. Yelton,[145] Y. R. Joshi,[146] S. Linn,[146] P. Markowitz,[146] J. L. Rodriguez,[146] A. Ackert,[147] T. Adams,[147] A. Askew,[147] S. Hagopian,[147] V. Hagopian,[147] K. F. Johnson,[147] T. Kolberg,[147] G. Martinez,[147] T. Perry,[147] H. Prosper,[147] A. Saha,[147] A. Santra,[147] V. Sharma,[147] R. Yohay,[147] M. M. Baarmand,[148] V. Bhopatkar,[148] S. Colafranceschi,[148] M. Hohlmann,[148] D. Noonan,[148] T. Roy,[148] F. Yumiceva,[148] M. R. Adams,[149] L. Apanasevich,[149] D. Berry,[149] R. R. Betts,[149] R. Cavanaugh,[149] X. Chen,[149] O. Evdokimov,[149] C. E. Gerber,[149] D. A. Hangal,[149] D. J. Hofman,[149] K. Jung,[149] J. Kamin,[149] I. D. Sandoval Gonzalez,[149] M. B. Tonjes,[149] H. Trauger,[149] N. Varelas,[149] H. Wang,[149] Z. Wu,[149] J. Zhang,[149] B. Bilki,[150,lll]

W. Clarida,[150] K. Dilsiz,[150,mmm] S. Durgut,[150] R. P. Gandrajula,[150] M. Haytmyradov,[150] V. Khristenko,[150] J.-P. Merlo,[150] H. Mermerkaya,[150,nnn] A. Mestvirishvili,[150] A. Moeller,[150] J. Nachtman,[150] H. Ogul,[150,ooo] Y. Onel,[150] F. Ozok,[150,ppp] A. Penzo,[150] C. Snyder,[150] E. Tiras,[150] J. Wetzel,[150] K. Yi,[150] B. Blumenfeld,[151] A. Cocoros,[151] N. Eminizer,[151] D. Fehling,[151] L. Feng,[151] A. V. Gritsan,[151] P. Maksimovic,[151] J. Roskes,[151] U. Sarica,[151] M. Swartz,[151] M. Xiao,[151] C. You,[151] A. Al-bataineh,[152] P. Baringer,[152] A. Bean,[152] S. Boren,[152] J. Bowen,[152] J. Castle,[152] S. Khalil,[152] A. Kropivnitskaya,[152] D. Majumder,[152] W. Mcbrayer,[152] M. Murray,[152] C. Rogan,[152] C. Royon,[152] S. Sanders,[152] E. Schmitz,[152] J. D. Tapia Takaki,[152] Q. Wang,[152] A. Ivanov,[153] K. Kaadze,[153] Y. Maravin,[153] A. Mohammadi,[153] L. K. Saini,[153] N. Skhirtladze,[153] F. Rebassoo,[154] D. Wright,[154] C. Anelli,[155] A. Baden,[155] O. Baron,[155] A. Belloni,[155] S. C. Eno,[155] Y. Feng,[155] C. Ferraioli,[155] N. J. Hadley,[155] S. Jabeen,[155] G. Y. Jeng,[155] R. G. Kellogg,[155] J. Kunkle,[155] A. C. Mignerey,[155] F. Ricci-Tam,[155] Y. H. Shin,[155] A. Skuja,[155] S. C. Tonwar,[155] D. Abercrombie,[156] B. Allen,[156] V. Azzolini,[156] R. Barbieri,[156] A. Baty,[156] R. Bi,[156] S. Brandt,[156] W. Busza,[156] I. A. Cali,[156] M. D'Alfonso,[156] Z. Demiragli,[156] G. Gomez Ceballos,[156] M. Goncharov,[156] D. Hsu,[156] M. Hu,[156] Y. Iiyama,[156] G. M. Innocenti,[156] M. Klute,[156] D. Kovalskyi,[156] Y.-J. Lee,[156] A. Levin,[156] P. D. Luckey,[156] B. Maier,[156] A. C. Marini,[156] C. Mcginn,[156] C. Mironov,[156] S. Narayanan,[156] X. Niu,[156] C. Paus,[156] C. Roland,[156] G. Roland,[156] J. Salfeld-Nebgen,[156] G. S. F. Stephans,[156] K. Tatar,[156] D. Velicanu,[156] J. Wang,[156] T. W. Wang,[156] B. Wyslouch,[156] A. C. Benvenuti,[157] R. M. Chatterjee,[157] A. Evans,[157] P. Hansen,[157] J. Hiltbrand,[157] S. Kalafut,[157] Y. Kubota,[157] Z. Lesko,[157] J. Mans,[157] S. Nourbakhsh,[157] N. Ruckstuhl,[157] R. Rusack,[157] J. Turkewitz,[157] M. A. Wadud,[157] J. G. Acosta,[158] S. Oliveros,[158] E. Avdeeva,[159] K. Bloom,[159] D. R. Claes,[159] C. Fangmeier,[159] F. Golf,[159] R. Gonzalez Suarez,[159] R. Kamalieddin,[159] I. Kravchenko,[159] J. Monroy,[159] J. E. Siado,[159] G. R. Snow,[159] B. Stieger,[159] J. Dolen,[160] A. Godshalk,[160] C. Harrington,[160] I. Iashvili,[160] D. Nguyen,[160] A. Parker,[160] S. Rappoccio,[160] B. Roozbahani,[160] G. Alverson,[161] E. Barberis,[161] C. Freer,[161] A. Hortiangtham,[161] A. Massironi,[161] D. M. Morse,[161] T. Orimoto,[161] R. Teixeira De Lima,[161] D. Trocino,[161] T. Wamorkar,[161] B. Wang,[161] A. Wisecarver,[161] D. Wood,[161] S. Bhattacharya,[162] O. Charaf,[162] K. A. Hahn,[162] N. Mucia,[162] N. Odell,[162] M. H. Schmitt,[162] K. Sung,[162] M. Trovato,[162] M. Velasco,[162] R. Bucci,[163] N. Dev,[163] M. Hildreth,[163] K. Hurtado Anampa,[163] C. Jessop,[163] D. J. Karmgard,[163] N. Kellams,[163] K. Lannon,[163] W. Li,[163] N. Loukas,[163] N. Marinelli,[163] F. Meng,[163] C. Mueller,[163] Y. Musienko,[163,ii] M. Planer,[163] A. Reinsvold,[163] R. Ruchti,[163] P. Siddireddy,[163] G. Smith,[163] S. Taroni,[163] M. Wayne,[163] A. Wightman,[163] M. Wolf,[163] A. Woodard,[163] J. Alimena,[164] L. Antonelli,[164] B. Bylsma,[164] L. S. Durkin,[164] S. Flowers,[164] B. Francis,[164] A. Hart,[164] C. Hill,[164] W. Ji,[164] B. Liu,[164] W. Luo,[164] B. L. Winer,[164] H. W. Wulsin,[164] S. Cooperstein,[165] O. Driga,[165] P. Elmer,[165] J. Hardenbrook,[165] P. Hebda,[165] S. Higginbotham,[165] A. Kalogeropoulos,[165] D. Lange,[165] J. Luo,[165] D. Marlow,[165] K. Mei,[165] I. Ojalvo,[165] J. Olsen,[165] C. Palmer,[165] P. Piroué,[165] D. Stickland,[165] C. Tully,[165] S. Malik,[166] S. Norberg,[166] A. Barker,[167] V. E. Barnes,[167] S. Das,[167] S. Folgueras,[167] L. Gutay,[167] M. K. Jha,[167] M. Jones,[167] A. W. Jung,[167] A. Khatiwada,[167] D. H. Miller,[167] N. Neumeister,[167] C. C. Peng,[167] H. Qiu,[167] J. F. Schulte,[167] J. Sun,[167] F. Wang,[167] R. Xiao,[167] W. Xie,[167] T. Cheng,[168] N. Parashar,[168] J. Stupak,[168] Z. Chen,[169] K. M. Ecklund,[169] S. Freed,[169] F. J. M. Geurts,[169] M. Guilbaud,[169] M. Kilpatrick,[169] W. Li,[169] B. Michlin,[169] B. P. Padley,[169] J. Roberts,[169] J. Rorie,[169] W. Shi,[169] Z. Tu,[169] J. Zabel,[169] A. Zhang,[169] A. Bodek,[170] P. de Barbaro,[170] R. Demina,[170] Y. t. Duh,[170] T. Ferbel,[170] M. Galanti,[170] A. Garcia-Bellido,[170] J. Han,[170] O. Hindrichs,[170] A. Khukhunaishvili,[170] K. H. Lo,[170] P. Tan,[170] M. Verzetti,[170] R. Ciesielski,[171] K. Goulianos,[171] C. Mesropian,[171] A. Agapitos,[172] J. P. Chou,[172] Y. Gershtein,[172] T. A. Gómez Espinosa,[172] E. Halkiadakis,[172] M. Heindl,[172] E. Hughes,[172] S. Kaplan,[172] R. Kunnawalkam Elayavalli,[172] S. Kyriacou,[172] A. Lath,[172] R. Montalvo,[172] K. Nash,[172] M. Osherson,[172] H. Saka,[172] S. Salur,[172] S. Schnetzer,[172] D. Sheffield,[172] S. Somalwar,[172] R. Stone,[172] S. Thomas,[172] P. Thomassen,[172] M. Walker,[172] A. G. Delannoy,[173] J. Heideman,[173] G. Riley,[173] K. Rose,[173] S. Spanier,[173] K. Thapa,[173] O. Bouhali,[174,qqq] A. Castaneda Hernandez,[174,qqq] A. Celik,[174] M. Dalchenko,[174] M. De Mattia,[174] A. Delgado,[174] S. Dildick,[174] R. Eusebi,[174] J. Gilmore,[174] T. Huang,[174] T. Kamon,[174,rrr] R. Mueller,[174] Y. Pakhotin,[174] R. Patel,[174] A. Perloff,[174] L. Perniè,[174] D. Rathjens,[174] A. Safonov,[174] A. Tatarinov,[174] K. A. Ulmer,[174] N. Akchurin,[175] J. Damgov,[175] F. De Guio,[175] P. R. Dudero,[175] J. Faulkner,[175] E. Gurpinar,[175] S. Kunori,[175] K. Lamichhane,[175] S. W. Lee,[175] T. Libeiro,[175] T. Mengke,[175] S. Muthumuni,[175] T. Peltola,[175] S. Undleeb,[175] I. Volobouev,[175] Z. Wang,[175] S. Greene,[176] A. Gurrola,[176] R. Janjam,[176] W. Johns,[176] C. Maguire,[176] A. Melo,[176] H. Ni,[176] K. Padeken,[176] P. Sheldon,[176] S. Tuo,[176] J. Velkovska,[176] Q. Xu,[176] M. W. Arenton,[177] P. Barria,[177] B. Cox,[177] R. Hirosky,[177] M. Joyce,[177] A. Ledovskoy,[177] H. Li,[177] C. Neu,[177] T. Sinthuprasith,[177] Y. Wang,[177] E. Wolfe,[177] F. Xia,[177] R. Harr,[178] P. E. Karchin,[178] N. Poudyal,[178] J. Sturdy,[178] P. Thapa,[178] S. Zaleski,[178] M. Brodski,[179] J. Buchanan,[179] C. Caillol,[179] S. Dasu,[179] L. Dodd,[179] S. Duric,[179] B. Gomber,[179] M. Grothe,[179]

M. Herndon,[179] A. Hervé,[179] U. Hussain,[179] P. Klabbers,[179] A. Lanaro,[179] A. Levine,[179] K. Long,[179] R. Loveless,[179] T. Ruggles,[179] A. Savin,[179] N. Smith,[179] W. H. Smith,[179] D. Taylor,[179] and N. Woods[179]

(CMS Collaboration)

[1]*Yerevan Physics Institute, Yerevan, Armenia*
[2]*Institut für Hochenergiephysik, Wien, Austria*
[3]*Institute for Nuclear Problems, Minsk, Belarus*
[4]*Universiteit Antwerpen, Antwerpen, Belgium*
[5]*Vrije Universiteit Brussel, Brussel, Belgium*
[6]*Université Libre de Bruxelles, Bruxelles, Belgium*
[7]*Ghent University, Ghent, Belgium*
[8]*Université Catholique de Louvain, Louvain-la-Neuve, Belgium*
[9]*Centro Brasileiro de Pesquisas Fisicas, Rio de Janeiro, Brazil*
[10]*Universidade do Estado do Rio de Janeiro, Rio de Janeiro, Brazil*
[11a]*Universidade Estadual Paulista, São Paulo, Brazil*
[11b]*Universidade Federal do ABC, São Paulo, Brazil*
[12]*Institute for Nuclear Research and Nuclear Energy, Bulgarian Academy of Sciences, Sofia, Bulgaria*
[13]*University of Sofia, Sofia, Bulgaria*
[14]*Beihang University, Beijing, China*
[15]*Institute of High Energy Physics, Beijing, China*
[16]*State Key Laboratory of Nuclear Physics and Technology, Peking University, Beijing, China*
[17]*Tsinghua University, Beijing, China*
[18]*Universidad de Los Andes, Bogota, Colombia*
[19]*University of Split, Faculty of Electrical Engineering, Mechanical Engineering and Naval Architecture, Split, Croatia*
[20]*University of Split, Faculty of Science, Split, Croatia*
[21]*Institute Rudjer Boskovic, Zagreb, Croatia*
[22]*University of Cyprus, Nicosia, Cyprus*
[23]*Charles University, Prague, Czech Republic*
[24]*Universidad San Francisco de Quito, Quito, Ecuador*
[25]*Academy of Scientific Research and Technology of the Arab Republic of Egypt, Egyptian Network of High Energy Physics, Cairo, Egypt*
[26]*National Institute of Chemical Physics and Biophysics, Tallinn, Estonia*
[27]*Department of Physics, University of Helsinki, Helsinki, Finland*
[28]*Helsinki Institute of Physics, Helsinki, Finland*
[29]*Lappeenranta University of Technology, Lappeenranta, Finland*
[30]*IRFU, CEA, Université Paris-Saclay, Gif-sur-Yvette, France*
[31]*Laboratoire Leprince-Ringuet, Ecole polytechnique, CNRS/IN2P3, Université Paris-Saclay, Palaiseau, France*
[32]*Université de Strasbourg, CNRS, IPHC UMR 7178, F-67000 Strasbourg, France*
[33]*Centre de Calcul de l'Institut National de Physique Nucleaire et de Physique des Particules, CNRS/IN2P3, Villeurbanne, France*
[34]*Université de Lyon, Université Claude Bernard Lyon 1, CNRS-IN2P3, Institut de Physique Nucléaire de Lyon, Villeurbanne, France*
[35]*Georgian Technical University, Tbilisi, Georgia*
[36]*Tbilisi State University, Tbilisi, Georgia*
[37]*RWTH Aachen University, I. Physikalisches Institut, Aachen, Germany*
[38]*RWTH Aachen University, III. Physikalisches Institut A, Aachen, Germany*
[39]*RWTH Aachen University, III. Physikalisches Institut B, Aachen, Germany*
[40]*Deutsches Elektronen-Synchrotron, Hamburg, Germany*
[41]*University of Hamburg, Hamburg, Germany*
[42]*Institut für Experimentelle Kernphysik, Karlsruhe, Germany*
[43]*Institute of Nuclear and Particle Physics (INPP), NCSR Demokritos, Aghia Paraskevi, Greece*
[44]*National and Kapodistrian University of Athens, Athens, Greece*
[45]*National Technical University of Athens, Athens, Greece*
[46]*University of Ioánnina, Ioánnina, Greece*
[47]*MTA-ELTE Lendület CMS Particle and Nuclear Physics Group, Eötvös Loránd University, Budapest, Hungary*

[48]*Wigner Research Centre for Physics, Budapest, Hungary*

[49]*Institute of Nuclear Research ATOMKI, Debrecen, Hungary*

[50]*Institute of Physics, University of Debrecen, Debrecen, Hungary*

[51]*Indian Institute of Science (IISc), Bangalore, India*

[52]*National Institute of Science Education and Research, Bhubaneswar, India*

[53]*Panjab University, Chandigarh, India*

[54]*University of Delhi, Delhi, India*

[55]*Saha Institute of Nuclear Physics, HBNI, Kolkata,India*

[56]*Indian Institute of Technology Madras, Madras, India*

[57]*Bhabha Atomic Research Centre, Mumbai, India*

[58]*Tata Institute of Fundamental Research-A, Mumbai, India*

[59]*Tata Institute of Fundamental Research-B, Mumbai, India*

[60]*Indian Institute of Science Education and Research (IISER), Pune, India*

[61]*Institute for Research in Fundamental Sciences (IPM), Tehran, Iran*

[62]*University College Dublin, Dublin, Ireland*

[63a]*INFN Sezione di Bari, Bari, Italy*

[63b]*Università di Bari, Bari, Italy*

[63c]*Politecnico di Bari, Bari, Italy*

[64a]*INFN Sezione di Bologna, Bologna, Italy*

[64b]*Università di Bologna, Bologna, Italy*

[65a]*INFN Sezione di Catania, Catania, Italy*

[65b]*Università di Catania, Catania, Italy*

[66a]*INFN Sezione di Firenze, Firenze, Italy*

[66b]*Università di Firenze, Firenze, Italy*

[67]*INFN Laboratori Nazionali di Frascati, Frascati, Italy*

[68a]*INFN Sezione di Genova, Genova, Italy*

[68b]*Università di Genova, Genova, Italy*

[69a]*INFN Sezione di Milano-Bicocca*

[69b]*Università di Milano-Bicocca*

[70a]*INFN Sezione di Napoli, Roma, Italy*

[70b]*Università di Napoli 'Federico II', Roma, Italy*

[70c]*Università della Basilicata, Roma, Italy*

[70d]*Università G. Marconi, Roma, Italy*

[71a]*INFN Sezione di Padova, Trento, Italy*

[71b]*Università di Padova, Trento, Italy*

[71c]*Università di Trento, Trento, Italy*

[72a]*INFN Sezione di Pavia, Pavia, Italy*

[72b]*Università di Pavia, Pavia, Italy*

[73a]*INFN Sezione di Perugia, Perugia, Italy*

[73b]*Università di Perugia, Perugia, Italy*

[74a]*INFN Sezione di Pisa, Pisa, Italy*

[74b]*Università di Pisa, Pisa, Italy*

[74c]*Scuola Normale Superiore di Pisa, Pisa, Italy*

[75a]*INFN Sezione di Roma, Rome, Italy*

[75b]*Sapienza Università di Roma, Rome, Italy*

[76a]*INFN Sezione di Torino, Novara, Italy*

[76b]*Università di Torino, Novara, Italy*

[76c]*Università del Piemonte Orientale, Novara, Italy*

[77a]*INFN Sezione di Trieste, Trieste, Italy*

[77b]*Università di Trieste, Trieste, Italy*

[78]*Kyungpook National University, Daegu, Korea*

[79]*Chonbuk National University, Jeonju, Korea*

[80]*Chonnam National University, Institute for Universe and Elementary Particles, Kwangju, Korea*

[81]*Hanyang University, Seoul, Korea*

[82]*Korea University, Seoul, Korea*

[83]*Seoul National University, Seoul, Korea*

[84]*University of Seoul, Seoul, Korea*

[85]*Sungkyunkwan University, Suwon, Korea*

[86]*Vilnius University, Vilnius, Lithuania*

[87]*National Centre for Particle Physics, Universiti Malaya, Kuala Lumpur, Malaysia*

[88]Centro de Investigacion y de Estudios Avanzados del IPN, Mexico City, Mexico

[89]Universidad Iberoamericana, Mexico City, Mexico

[90]Benemerita Universidad Autonoma de Puebla, Puebla, Mexico

[91]Universidad Autónoma de San Luis Potosí, San Luis Potosí, Mexico

[92]University of Auckland, Auckland, New Zealand

[93]University of Canterbury, Christchurch, New Zealand

[94]National Centre for Physics, Quaid-I-Azam University, Islamabad, Pakistan

[95]National Centre for Nuclear Research, Swierk, Poland

[96]Institute of Experimental Physics, Faculty of Physics, University of Warsaw, Warsaw, Poland

[97]Laboratório de Instrumentação e Física Experimental de Partículas, Lisboa, Portugal

[98]Joint Institute for Nuclear Research, Dubna, Russia

[99]Petersburg Nuclear Physics Institute, Gatchina (St. Petersburg), Russia

[100]Institute for Nuclear Research, Moscow, Russia

[101]Institute for Theoretical and Experimental Physics, Moscow, Russia

[102]Moscow Institute of Physics and Technology, Moscow, Russia

[103]National Research Nuclear University 'Moscow Engineering Physics Institute' (MEPhI),
Moscow, Russia

[104]P.N. Lebedev Physical Institute, Moscow, Russia

[105]Skobeltsyn Institute of Nuclear Physics, Lomonosov Moscow State University, Moscow, Russia

[106]Novosibirsk State University (NSU), Novosibirsk, Russia

[107]State Research Center of Russian Federation, Institute for High Energy Physics, Protvino, Russia

[108]University of Belgrade, Faculty of Physics and Vinca Institute of Nuclear Sciences, Belgrade, Serbia

[109]Centro de Investigaciones Energéticas Medioambientales y Tecnológicas (CIEMAT), Madrid, Spain

[110]Universidad Autónoma de Madrid, Madrid, Spain

[111]Universidad de Oviedo, Oviedo, Spain

[112]Instituto de Física de Cantabria (IFCA), CSIC-Universidad de Cantabria, Santander, Spain

[113]CERN, European Organization for Nuclear Research, Geneva, Switzerland

[114]Paul Scherrer Institut, Villigen, Switzerland

[115]ETH Zurich—Institute for Particle Physics and Astrophysics (IPA), Zurich, Switzerland

[116]Universität Zürich, Zurich, Switzerland

[117]National Central University, Chung-Li, Taiwan

[118]National Taiwan University (NTU), Taipei, Taiwan

[119]Chulalongkorn University, Faculty of Science, Department of Physics, Bangkok, Thailand

[120]Çukurova University, Physics Department, Science and Art Faculty, Adana, Turkey

[121]Middle East Technical University, Physics Department, Ankara, Turkey

[122]Bogazici University, Istanbul, Turkey

[123]Istanbul Technical University, Istanbul, Turkey

[124]Institute for Scintillation Materials of National Academy of Science of Ukraine, Kharkov, Ukraine

[125]National Scientific Center, Kharkov Institute of Physics and Technology, Kharkov, Ukraine

[126]University of Bristol, Bristol, United Kingdom

[127]Rutherford Appleton Laboratory, Didcot, United Kingdom

[128]Imperial College, London, United Kingdom

[129]Brunel University, Uxbridge, United Kingdom

[130]Baylor University, Waco, USA

[131]Catholic University of America, Washington, USA

[132]The University of Alabama, Tuscaloosa, USA

[133]Boston University, Boston, USA

[134]Brown University, Providence, USA

[135]University of California, Davis, Davis, USA

[136]University of California, Los Angeles, USA

[137]University of California, Riverside, Riverside, USA

[138]University of California, San Diego, La Jolla, USA

[139]University of California, Santa Barbara—Department of Physics, Santa Barbara, USA

[140]California Institute of Technology, Pasadena, USA

[141]Carnegie Mellon University, Pittsburgh, USA

[142]University of Colorado Boulder, Boulder, USA

[143]Cornell University, Ithaca, USA

[144]Fermi National Accelerator Laboratory, Batavia, USA

[145]University of Florida, Gainesville, USA

[146]Florida International University, Miami, USA

[147]*Florida State University, Tallahassee, USA*
[148]*Florida Institute of Technology, Melbourne, USA*
[149]*University of Illinois at Chicago (UIC), Chicago, USA*
[150]*The University of Iowa, Iowa City, USA*
[151]*Johns Hopkins University, Baltimore, USA*
[152]*The University of Kansas, Lawrence, USA*
[153]*Kansas State University, Manhattan, USA*
[154]*Lawrence Livermore National Laboratory, Livermore, USA*
[155]*University of Maryland, College Park, USA*
[156]*Massachusetts Institute of Technology, Cambridge, USA*
[157]*University of Minnesota, Minneapolis, USA*
[158]*University of Mississippi, Oxford, USA*
[159]*University of Nebraska-Lincoln, Lincoln, USA*
[160]*State University of New York at Buffalo, Buffalo, USA*
[161]*Northeastern University, Boston, USA*
[162]*Northwestern University, Evanston, USA*
[163]*University of Notre Dame, Notre Dame, USA*
[164]*The Ohio State University, Columbus, USA*
[165]*Princeton University, Princeton, USA*
[166]*University of Puerto Rico, Mayaguez, USA*
[167]*Purdue University, West Lafayette, USA*
[168]*Purdue University Northwest, Hammond, USA*
[169]*Rice University, Houston, USA*
[170]*University of Rochester, Rochester, USA*
[171]*The Rockefeller University, New York, USA*
[172]*Rutgers, The State University of New Jersey, Piscataway, USA*
[173]*University of Tennessee, Knoxville, USA*
[174]*Texas A&M University, College Station, USA*
[175]*Texas Tech University, Lubbock, USA*
[176]*Vanderbilt University, Nashville, USA*
[177]*University of Virginia, Charlottesville, USA*
[178]*Wayne State University, Detroit, USA*
[179]*University of Wisconsin—Madison, Madison, Wisconsin, USA*

[a]Deceased.
[b]Also at Vienna University of Technology, Vienna, Austria.
[c]Also at IRFU, CEA, Université Paris-Saclay, Gif-sur-Yvette, France.
[d]Also at Universidade Estadual de Campinas, Campinas, Brazil.
[e]Also at Universidade Federal de Pelotas, Pelotas, Brazil.
[f]Also at Université Libre de Bruxelles, Bruxelles, Belgium.
[g]Also at Institute for Theoretical and Experimental Physics, Moscow, Russia.
[h]Also at Joint Institute for Nuclear Research, Dubna, Russia.
[i]Also at Suez University, Suez, Egypt.
[j]Also at British University in Egypt, Cairo, Egypt.
[k]Also at Helwan University, Cairo, Egypt.
[l]Also at Université de Haute Alsace, Mulhouse, France.
[m]Also at Skobeltsyn Institute of Nuclear Physics, Lomonosov Moscow State University, Moscow, Russia.
[n]Also at CERN, European Organization for Nuclear Research, Geneva, Switzerland.
[o]Also at RWTH Aachen University, III. Physikalisches Institut A, Aachen, Germany.
[p]Also at University of Hamburg, Hamburg, Germany.
[q]Also at Brandenburg University of Technology, Cottbus, Germany.
[r]Also at MTA-ELTE Lendület CMS Particle and Nuclear Physics Group, Eötvös Loránd University, Budapest, Hungary.
[s]Also at Institute of Nuclear Research ATOMKI, Debrecen, Hungary.
[t]Also at Institute of Physics, University of Debrecen, Debrecen, Hungary.
[u]Also at IIT Bhubaneswar, Bhubaneswar, India.
[v]Also at Institute of Physics, Bhubaneswar, India.
[w]Also at University of Visva-Bharati, Santiniketan, India.
[x]Also at University of Ruhuna, Matara, Sri Lanka.
[y]Also at Isfahan University of Technology, Isfahan, Iran.
[z]Also at Yazd University, Yazd, Iran.

[aa]Also at Plasma Physics Research Center, Science and Research Branch, Islamic Azad University, Tehran, Iran.

[bb]Also at Università degli Studi di Siena, Siena, Italy.

[cc]Also at INFN Sezione di Milano-Bicocca, Università di Milano-Bicocca, Milano, Italy.

[dd]Also at Purdue University, West Lafayette, USA.

[ee]Also at International Islamic University of Malaysia, Kuala Lumpur, Malaysia.

[ff]Also at Malaysian Nuclear Agency, MOSTI, Kajang, Malaysia.

[gg]Also at Consejo Nacional de Ciencia y Tecnología, Mexico city, Mexico.

[hh]Also at Warsaw University of Technology, Institute of Electronic Systems, Warsaw, Poland.

[ii]Also at Institute for Nuclear Research, Moscow, Russia.

[jj]Also at National Research Nuclear University 'Moscow Engineering Physics Institute' (MEPhI), Moscow, Russia.

[kk]Also at St. Petersburg State Polytechnical University, St. Petersburg, Russia.

[ll]Also at University of Florida, Gainesville, USA.

[mm]Also at P.N. Lebedev Physical Institute, Moscow, Russia.

[nn]Also at California Institute of Technology, Pasadena, USA.

[oo]Also at Budker Institute of Nuclear Physics, Novosibirsk, Russia.

[pp]Also at Faculty of Physics, University of Belgrade, Belgrade, Serbia.

[qq]Also at University of Belgrade, Faculty of Physics and Vinca Institute of Nuclear Sciences, Belgrade, Serbia.

[rr]Also at Scuola Normale e Sezione dell'INFN, Pisa, Italy.

[ss]Also at National and Kapodistrian University of Athens, Athens, Greece.

[tt]Also at Riga Technical University, Riga, Latvia.

[uu]Also at Universität Zürich, Zurich, Switzerland.

[vv]Also at Stefan Meyer Institute for Subatomic Physics.

[ww]Also at Gaziosmanpasa University, Tokat, Turkey.

[xx]Also at Istanbul Aydin University, Istanbul, Turkey.

[yy]Also at Mersin University, Mersin, Turkey.

[zz]Also at Cag University, Mersin, Turkey.

[aaa]Also at Piri Reis University, Istanbul, Turkey.

[bbb]Also at Adiyaman University, Adiyaman, Turkey.

[ccc]Also at Izmir Institute of Technology, Izmir, Turkey.

[ddd]Also at Necmettin Erbakan University, Konya, Turkey.

[eee]Also at Marmara University, Istanbul, Turkey.

[fff]Also at Kafkas University, Kars, Turkey.

[ggg]Also at Istanbul Bilgi University, Istanbul, Turkey.

[hhh]Also at Rutherford Appleton Laboratory, Didcot, United Kingdom.

[iii]Also at School of Physics and Astronomy, University of Southampton, Southampton, United Kingdom.

[jjj]Also at Instituto de Astrofísica de Canarias, La Laguna, Spain.

[kkk]Also at Utah Valley University, Orem, USA.

[lll]Also at Beykent University.

[mmm]Also at Bingol University, Bingol, Turkey.

[nnn]Also at Erzincan University, Erzincan, Turkey.

[ooo]Also at Sinop University, Sinop, Turkey.

[ppp]Also at Mimar Sinan University, Istanbul, Istanbul, Turkey.

[qqq]Also at Texas A&M University at Qatar, Doha, Qatar

[rrr]Also at Kyungpook National University, Daegu, Korea.